Quaternary Science Reviews 199 (2018) 188–205

Contents lists available at ScienceDirect

Quaternary Science Reviews

journal homepage: www.elsevier.com/locate/quascirev

A postglacial relative sea-level database for the Russian Arctic coast

Alisa V. Baranskaya [a, *], Nicole S. Khan [b], Fedor A. Romanenko [a], Keven Roy [b], W.R. Peltier [d], Benjamin P. Horton [b, c, e]

[a] Lomonosov Moscow State University, Laboratory of Geoecology of the North, Moscow, Russia
[b] Asian School of the Environment, Nanyang Technological University, Singapore, 639798, Singapore
[c] Earth Observatory of Singapore, Nanyang Technological University Singapore, 639798, Singapore
[d] Department of Physics, University of Toronto, Toronto, Canada
[e] Department of Marine and Coastal Sciences, Rutgers University, New Brunswick, NJ 08901, USA

ARTICLE INFO

Article history:
Received 31 March 2018
Received in revised form
15 July 2018
Accepted 21 July 2018
Available online 23 August 2018

Keywords:
Sea level changes
Russian arctic
Holocene
Data treatment
Data analysis
Glacial isostatic adjustment
Eustatic sea level
Vertical movements of the Earth's crust

ABSTRACT

We present the first quality-controlled relative sea-level (RSL) database for the Russian Arctic coast from the Barents Sea in the west to Laptev Sea in the east (29–152°E and 63 to 81°N). The database consists of 385 sea-level index points and 249 limiting dates and spans 24 ka to present. Sea-level indicators are derived from multiple proxies, including isolation basins, raised beaches, glacial erratics, marine terraces, laidas (salt marshes), and deltaic salt marshes. Here, we calculate the indicative meanings for all indicators and evaluated possible elevation errors. We have estimated the ages and uncertainties of index points and limiting dates using the most recent calibration datasets.

In the western Russian Arctic (Barents and White Seas), RSL was driven by glacial isostatic adjustment (GIA) due to deglaciation of the Eurasian ice sheet complex. For example, within the Baltic crystalline shield, RSL fell rapidly from 80 to 100 m at 11–12 ka to 15–25 m at ~4–5 ka. In the Arctic Islands of Franz-Joseph Land and Novaya Zemlya, RSL gradually fell from 25 to 35 m at 9 ka to 5–10 m at 3 ka. The Timan coast and the Kara Sea shelf are characterized by constant RSL rise due to proglacial forebulge collapse; Yamal and the Gydan Peninsula and Novaya Zemlya are all marked by a high LGM position of RSL, followed by a lowstand and consequent rise to a late Holocene highstand of several meters. Data from the Laptev Sea coasts and shelf and the New Siberian Islands demonstrate post-LGM RSL rise with a Holocene highstand of up to 5–10 m, with scatter caused by differential tectonic movements along a diffuse lithospheric plate boundary. The collected database allowed to estimate and discuss the reasons of both spatial and temporal variability of RSL histories in different parts of the Russian Arctic.

1. Introduction

Changes in relative sea level (RSL) of the Russian Arctic since the Last Glacial Maximum (LGM) can provide important insights into the development of polar regions since deglaciation (Kaplin and Selivanov, 1999). RSL changes provide evidence of palaeogeographic conditions (Møller et al., 2002), deglaciation chronology and mechanisms (Forman et al., 1996; Kolka et al., 2013a), the source of meltwater contributions (e.g., Clark et al., 2002), and spatial and temporal variability of glacio-isostatic adjustment (GIA) due to changing ice mass loads (Lambeck et al., 2002; Forman et al., 2004; Peltier, 2004). It follows that RSL records from the Russian Arctic seas provide constraints on Earth's rheology, as well as on rates of modern tectonic uplift or subsidence (Kolka et al., 2013b; Koshechkin, 1979).

The spatial variability of RSL change in the Russian Arctic is caused by vertical land motion (Proshutinsky et al., 2004), imposed on a eustatic sea-level trend (e.g., Lambeck et al., 2014). Vertical land motion is dominated by GIA, especially in the western part of Russian Arctic (Kaplin and Selivanov, 1999). At the LGM, the growth of the Eurasian ice sheet complex, formed from the Britain and Ireland, Scandinavian, and the Barents-Kara nucleation centers (Patton et al., 2017), caused subsidence in the center of ice loading and uplift of a compensational forebulge near ice margins (Ekman and Mäkinen, 1996; Peltier, 2004; Peltier et al., 1978, 2015). During deglaciation, lithospheric rebound in formerly glaciated territories resulted in uplift of the Baltic crystalline shield (Corner et al., 1999,

* Corresponding author. Laboratory of geoecology of the North, Faculty of Geography, Lomonosov Moscow State University, GSP-1, Leninskie Gory, Moscow, 119991, Russia.
E-mail address: alisa.baranskaya@yandex.ru (A.V. Baranskaya).

https://doi.org/10.1016/j.quascirev.2018.07.033
0277-3791/

2001; Møller et al., 2002; Snyder et al., 1997), Franz-Josef Land (Forman et al., 1995; 1996, 2004) and Novaya Zemlya (Forman et al., 1995; 1999, 2004; Zeeberg et al., 2001). In the early Holocene, the forebulge near the former ice margins subsided, as the mantle readjusted during relaxation (Ekman and Mäkinen, 1996; Peltier, 2004). In the mid-Holocene, GIA-induced vertical movements decelerated, although they are still an important component of modern RSL variability in the western part of the Russian Arctic (Forman et al., 1995; 1996, 2004; Kolka et al., 2005).

The complex tectonic setting of the Russian Arctic also influences vertical land motion (Drachev, 2016; Pease et al., 2014). Modern and Holocene active seismicity have been documented in the Laptev Sea rift system (Drachev et al., 2003) and in the western part of the Russian Arctic (Imaev et al., 1995; Konechnaya, 2013; Nikolaeva et al., 2007; Vinogradov et al., 2006), complicating the attribution of land motion to GIA.

RSL records from the Russian Arctic provide constraints on the vertical land motion from GIA and/or tectonics (Milne et al., 2009); however, postglacial RSL studies are scarce, and neither quality control nor considerations of uncertainty have been implemented in the existing analyses (Baranskaya, 2015; Makarov, 2017). Here, we present the first quality-controlled database of postglacial RSL changes from 24 ka to present covering the Russian Arctic coasts and shelf from the Barents and White Seas in the west to Laptev Sea in the east (Figs. 1 and 2). We define the indicative meanings and ages of multiple sea-level indicators, including isolation basins,

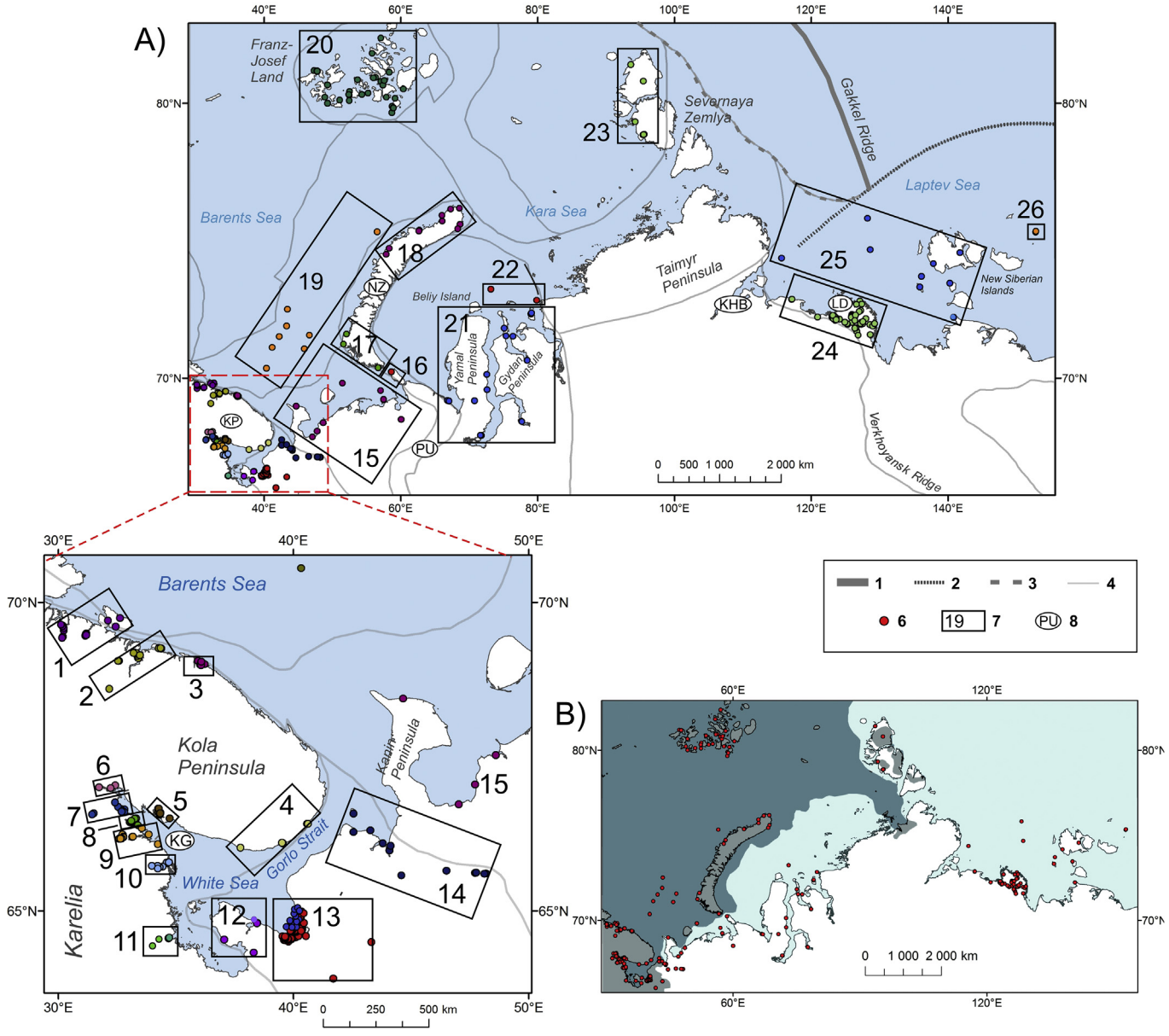

Fig. 1. A) Spatial distribution of the Russian Arctic sea-level data. 1 - active spreading axis; 2 – Khatanga-Lomonosov transform fault; 3 - approximated limit of continent-ocean transition zone; 4 - borders of simplified tectonic structures; 5 - sea-level points from the database; 6 - sea-level regions and their numbers (1 - Murman Coast 1, 2 - Murman Coast 2, 3 - Murman Coast 3, 4 - Eastern Kola Peninsula, 5 - Umba, 6 - Kandalaksha, 7 - Lesozavodskiy, 8 - Rugozerskiy Peninsula, 9 - Chupa Bay and Keret archipelago, 10 - Engozero, 11 - Belomorsk, 12 - Onega Peninsula, 13 - Dvina Gulf, 14 - Mezen Gulf, 15 - Timan Coast, 16 - Vaygach Island, 17 - Novaya Zemlya South Island, 18 - Novaya Zemlya North Island, 19 - Barents Sea shelf, 20 - Franz-Josef Land, 21 - Yamal and Gydan Peninsula, 22 - Kara Sea shelf, 23 - Severnaya Zemlya, 24 - Lena Delta and Laptev Sea coasts, 25 - Laptev Sea shelf and western New Siberian Islands, 26 - Zhokhov Island); 7 - geographic names: PU - Polar Ural, KP - Kola Peninsula, NZ - Novaya Zemlya, KHB - Khatanga Bay, BH - Buor Khaya Bay, LD - Lena Delta, KG - Kandalaksha Gulf; B) Limits of the Eurasian ice sheet at its LGM maximum extent (after Patton et al., 2017) shown in grey; red dots indicate points from the RSL database.

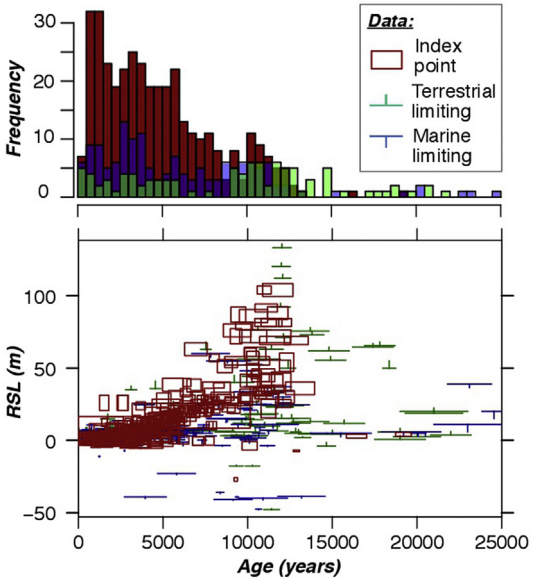

Fig. 2. Temporal distribution of the Russian Arctic sea-level data. On the histogram, red bars indicate index points; blue bars indicate marine limiting points and green bars indicate terrestrial limiting points.

raised beaches, glacial erratics, marine terraces, laidas, and deltaic salt marshes and muds. We examine the magnitude and geographic variability of RSL change (and its associated uncertainty) and review the mechanisms driving these spatial patterns.

2. Study area

The compiled database covers the coasts and shelf of the White, Barents, Kara and Laptev Seas. Given the wide spatial coverage of the database, and the possibility of strong gradients in land-level change caused by ice-sheet dynamics and tectonics, it was divided into 26 regions, based on: a) location; b) relative influence of GIA; c) tectonic setting; and d) local geomorphological conditions.

2.1. Baltic shield (Regions 1–11)

The Baltic shield is situated in northwest Russia and includes the Kola Peninsula and northern and central Karelia (Fig. 3). In the west, it continues further into Finland, Sweden and Norway. Geologically it is part of the Early Pre-Cambrian East European (or Russian) Platform basement composed of igneous and metamorphic Archaean and Proterozoic rocks (Slabunov et al., 2006; Mints et al., 2015).

The modern tectonics of the Baltic shield are determined by the re-activation of numerous Pre-Cambrian faults. In the north, the shield is separated from the Barents Sea by a large fault zone stretching along the Murmansk (northeastern) coast of the Kola Peninsula called Karpinskiy Lineament in its Russian sector (Lukashov and Romanenko, 2010) (Fig. 3). It is expressed as a system of young normal faults extending along the northern margin of the Kola Peninsula, and is the boundary between the shield and a region of the East European Craton pericratonic subsidence (Baluev et al., 2016). In the southeast, the Baltic Shield is cut by the White Sea Rift system, which formed in the Neoproterozoic time and was reactivated during the Neotectonic stage (Late Cenozoic). At that time, the rift system developed further to the northwest, creating modern active faults and grabens (Baluev et al., 2009 a; b). The territory of the Baltic shield is characterized by modern seismicity (Vinogradov et al., 2006), which may have been more active during the Holocene (Nikolaeva et al., 2007; Nikolaeva, 2016).

In the Pleistocene, the Baltic shield was glaciated several times. The most recent LGM Scandinavian ice sheet was the largest by volume, with maximum thickness exceeding 2 km near the apex of the Kandalaksha Gulf (Clason et al., 2014; Svendsen et al., 2004). It retreated in several stages from 16 to 11 ka (Demidov et al., 2006; Stroeven et al., 2016). GIA subsequently resulted in rapid uplift of the territory, with rates reaching 20 m/ka at the beginning of the Holocene (Kolka et al., 2005).

2.2. Russian plate (Regions 12–14)

The Russian plate (Fig. 3) is also part of the Early Pre-Cambrian East European (or Russian) Platform (Mints et al., 2015). Its crystalline Archaean and Proterozoic basement is overlain by sedimentary cover, thickening to the southeast and cut by northwesterly faults and grabens, representing the continuation of the White Sea Rift system on land (Baluev et al., 2009a; b), which is associated with modern seismicity that is less frequent and intense than on the Baltic shield (Bogdanov et al., 2000).

The northern part of the Russian plate was glaciated several times during the Pleistocene. At the LGM, the Scandinavian Ice Sheet occupied the northwestern part of the Russian plate from 21 to 17 ka (Hughes et al., 2016). The limit of the glacial maximum runs from the White Sea shore of the Kanin peninsula to the southwest (Demidov et al., 2004, Fig. 1). Ice thickness in this area was smaller than on the Baltic shield and did not exceed 1200–1500 m (Clason et al., 2014).

2.3. Timan fold belt and Timan-Pechora Platform (Region 15)

The Timan fold belt is locally exposed on the Kanin Peninsula, and stretches as a narrow patch to the north of the Baltic shield (Drachev, 2016), while a major part of it is buried under the thick Paleozoic-Mesozoic sedimentary cover of the Timan-Pechora Platform (Fig. 3), which is considered to have been relatively stable during Neotectonic time. A narrow region of the East European Craton pericratonic subsidence stretches from the northwest to the southeast in its western part, bordered by the reverse–strike-slip zone of the Trollfjord– Rybachiy–Kanin Lineament (Baluev et al., 2016), also mentioned as the West Timanian Thrust (Drachev, 2016). This is a relatively old (Late Proterozoic - Middle Cambrian) fault zone, active in its western part close to the Kola Peninsula shore and hidden under a sedimentary cover in the east (Baluev et al., 2016).

Controversy exists over the extent and timing of the glaciations. While there is consensus that the Barents-Kara ice sheet covered the area several times during the Pleistocene, its spatial extent at the LGM remains disputed: outcrops on land suggest that the ice sheet moved as much as 150 km up the Pechora River (Arslanov et al., 1987; Lavrov and Potapenko, 2005); however, drilling of the Pechora Sea floor sediments suggests that the late Weichselian Barents-Kara ice sheet occupied the northwestern part of the Pechora Sea, but did not reach the coast of the Pechora lowland (Patton et al., 2017; Polyak et al., 2000; Svendsen et al., 2004). The glacial limit presumably ran around Kanin Peninsula, and further to the northeast (Patton et al., 2017; Svendsen et al., 2004).

2.4. Ural-Novaya Zemlya fold belt (Regions 16–18)

The Ural-Novaya Zemlya Fold Belt is situated to the east of the Timan-Pechora platform (Fig. 3); it divides the European and Asian parts of the Russian Arctic. It is part of a former platform with Late

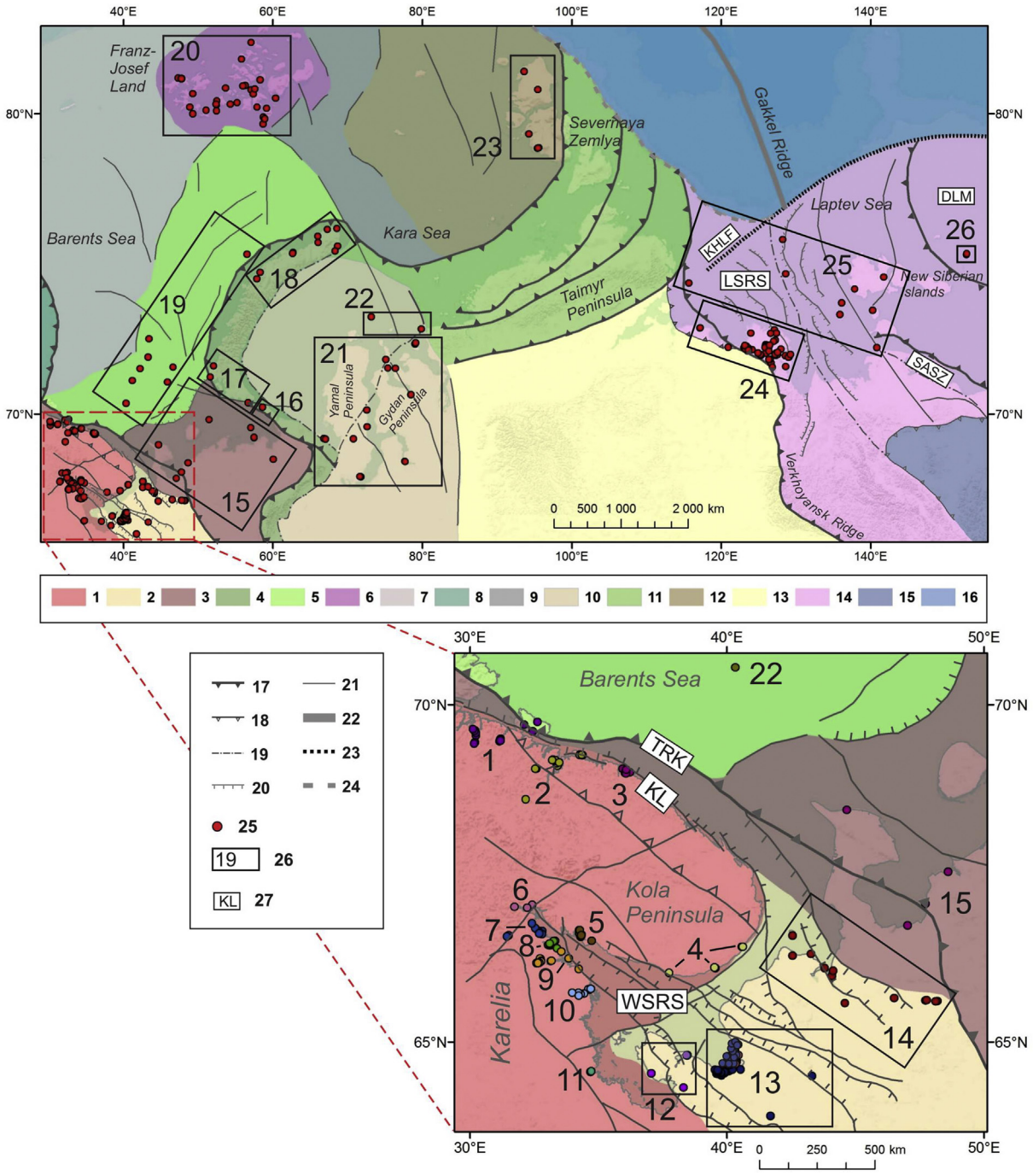

Fig. 3. Simplified tectonics of the Russian Arctic (after: Pease et al., 2014, Drachev, 2016, Baluev et al., 2009a, Baluev et al., 2016, Vernikovsky et al., 2013, integrated and generalized). The numbering of RSL regions is identical to Fig. 1. The color legend 1–16 refers to the main morpho-tectonic structures shown on the map in colors: 1 - Baltic Shield, 2 - Russian Plate, 3 - Timan fold belt and Timan-Pechora Platform, 4 - Ural-Novaya Zemlya fold belt, 5 - East Barents sea troughs, 6 - Franz-Josef Land flood basalt massive, 7 - Svalbard Plate, 8 - Scandinavian fold belt, 9 - St Anna trough and North Siberian step, 10 - West-Siberian Platform, 11 - Taimyr fold belt, 12 - Kara Plate, 13 - Siberian Platform (Siberian Craton), 14 - Laptev Sea continental margin, 15 - Kolyma fold belt (Kolyma loop), 16 - Eurasian oceanic basin. Faults: 17 - fold belt deformation front, 18 - thrust, 19 - suture, 20 - normal fault, 21 - other faults, 22 - active spreading axis, 23 - transform fault, 24 - approximated limit of continent-ocean transition zone; 25 - sea-level points from the database; 26 - sea-level regions and their numbers (same as in Fig. 1); 27 - faults' and tectonic structures' names: KL - Karpinskiy Lineament, TRK - Trollfjord–Rybachi–Kanin Lineament, WSRS - White Sea rift system, LSRS - Laptev Sea rift system, KHLF - Khatanga-Lomonosov transform fault, SASZ - South Anyui Suture Zone, DLM - De Long Massive.

Precambrian basement folded by Hercynian (Late Paleozoic) tectonic deformations (Vernikovsky et al., 2013). The Ural ridge continues northward to Vaygach Island (Region 16) and further to the South and to the North Island of Novaya Zemlya (Regions 17 and 18). In the Neotectonic time, the fold belt was characterized by moderate seismicity (Avetisov, 1996).

At the LGM, Novaya Zemlya was one of the centers of the Barents-Kara Ice sheet, and remained glaciated for some time after the ice retreated from the shelves (Hughes et al., 2016). The border of the LGM ice sheet lies immediately south from Novaya Zemlya (Fig. 1; Patton et al., 2017), suggesting that Vaygach Island (Region 16) was not covered by the ice sheet at the LGM.

2.5. East Barents sea (Region 19)

The floor of the central and northern Barents Sea is part of the Svalbard plate with Grenvillian (Mesoproterozoic) basement. In the east, it is dissected by deep tectonic troughs, such as the East Barents and St. Anna troughs, some of which presumably have an intermediate type of crust (i.e., transitional from continental to oceanic) (Vernikovsky et al., 2013) and may even be underlain by exhumed mantle or oceanic lithosphere (Drachev, 2016). In certain areas, the basement can lie at depths of up to 15 km (Burguto et al., 2016), implying active Neotectonic subsidence of the troughs (Krapivner, 2006).

During the LGM, the Barents shelf was completely covered by the Barents-Kara ice sheet (Patton et al., 2017).

2.6. Franz-Josef Land (Region 20)

Franz-Josef Land is situated within an anticline of the Svalbard plate, dissected by a Mesozoic trappean complex (Vernikovsky et al., 2013), which forms islands and plateaus up to 620 m high. Together with Novaya Zemlya, it was one of the centers of the Barents-Kara ice sheet at the LGM and currently experiences glacio-isostatic uplift (Forman et al., 2004). Modern local ice caps and glaciers are still preserved in its severe climate.

2.7. West Siberian Platform (Regions 21, 22)

The West Siberian Platform is a young plate with heterogeneous folded basement made by formations of mostly Paleozoic age, covered by Mesozoic and Cenozoic sediments of the West Siberian basin (Ivanov et al., 2016). In the north, the Kara Sea shelf is part of the Kara Plate and North Kara Basin (Afanasenkov et al., 2016).

The West Siberian platform was covered by ice sheets several times in the Pleistocene; however, the LGM ice sheet did not reach the coasts of Yamal and the Gydan Peninsula (Svendsen et al., 2004), where the last glaciation occurred no later than 60 ka (Forman et al., 2002).

2.8. Severnaya Zemlya (Region 23)

The Severnaya Zemlya (or North Land) orogen is part of the Taimyr orogen in the south, and a deformed part of the North Kara basin in the north (Afanasenkov et al., 2016). Both are characterized by a Precambrian basement with Paleozoic sedimentary cover, which was folded in Caledonian time (Early-Middle Palaeozoic).

During the LGM, the Barents-Kara ice sheet did not reach Severnaya Zemlya archipelago, although there is evidence of glacial cover in some areas of Taimyr (Drachev et al., 2003; Svendsen et al., 2004); however, local small ice sheets and mountain glaciers existed (Patton et al., 2017), and partly remain today.

2.9. Laptev Sea continental margin (Regions 24–26)

Geologically the territory of the southwestern Laptev Sea coasts (Region 24) belongs to the Verkhoyansk fold belt, a Paleozoic to Mesozoic passive margin of the eastern Siberian Palaeocontinent, folded in Late Jurassic and Early Cretaceous (Drachev, 2016) and continuing under the Lena Delta and Laptev shelf sedimentary cover (Drachev and Shkarubo, 2017).

The area of the south-western New Siberian Islands and adjacent shelf (eastern part of Region 25) has a heterogeneous tectonic structure. Generally, it consists of a Late Precambrian basement, partly deformed by Cimmerian tectonic deformations, dissected by young (Cretaceous-Neogene) basalts and other volcanic formations and cut by Mesozoic riftogenic basins (Vernikovsky et al., 2013). To the south, it is bordered by the South Anyui Suture zone, a middle Cretaceous collision fold-thrust system (Khain and Filatova, 2007) separating the New Siberian Islands from the Verkhoyansk fold belt.

The northeastern part of the New Siberian Islands archipelago (including Region 26) belongs to De Long Massive, also known in the Russian literature as the Hyperborean or East Arctic Platform, consisting of two terranes with heterogenuous structure formed at the latest during the Early Palaeozoic (Pease et al., 2014).

The Laptev Sea has the only active continental margin in the Russian Arctic, demarcating a transitional area from oceanic spreading to continental rifting. The mid-oceanic ultraslow spreading Gakkel ridge terminates against the northern border of the Laptev Sea shelf marked by the Lomonosov-Khatanga transform fault (Drachev et al., 2003). The area of extension shifts towards the west and continues further on the shelf as a series of subparallel rifts: namely the Belkov-Svyatoy Nos rift, the Ust-Lena rift, the Ust-Yana rift, etc, making together the Laptev Sea Rift System (western part of Region 25; Drachev, 1998). These rifts are seismically active (Imaev et al., 1995, 2000); there is evidence of modern displacement of Quaternary deposits above them. The seismic zone of the Laptev Sea rifts continues to the southeast on land (Hindle and Mackey, 2011), widening from the Laptev Sea and the mouth of the Lena River towards the Sea of Okhotsk. This structure is often interpreted as a “diffuse” margin of the North American and Eurasian plates (Hindle et al., 2006; Stein and Sella, 2002).

Coastal areas to the east and west of the plate boundary are also characterized by high Neotectonic (Cenozoic) seismicity (Imaev et al., 1995). In the Lena Delta, the same sedimentary units lie higher in the western part than in the east, suggesting differential vertical land movements since at least the Neo-Pleistocene. Further evidence of such differential movement is provided by changes in the Lena River runoff direction, which has shifted with time from the Olenyok channel in the west to the Bykovskaya channel in the east, due to uplift of the delta's western region (Grigoriev, 1993).

The southwestern part of the Laptev continental margin was never covered by Quaternary ice sheets, due to its dry continental climate (Svendsen et al., 2004). In the late Pleistocene, ice-rich permafrost, called Yedoma or Ice Complex, accumulated in tundra landscapes (Schirrmeister et al., 2011). Buried glacier ice found on the New Siberian Islands provides evidence of the existence of an ice sheet in the second half of the middle Neo-Pleistocene (84–135 ka) (Basilyan et al., 2010; Tumskoy, 2012). During the LGM, the territory was ice-free, and Ice Complex sequences accumulated in cold tundra-steppe landscapes (Wetterich et al., 2011).

3. The methodology employed to reconstruct RSL

For accurate estimation of RSL change, a precise and unified determination of sea-level indicators is necessary. We follow the standardized methodology developed by the International Geological Correlation Projects (IGCP) projects (e.g., Gehrels and Long, 2007; Hijma et al., 2015; Preuss, 1979; van de Plassche, 1995) to determine RSL, age, and associated uncertainties of sea-level index points, which define the varying position of RSL in time.

3.1. Sea-level indicators and their indicative meaning

The indicative meaning describes the relationship of the indicator to sea level at its time of formation. It has two components: the reference water level, which relates the central tendency of the indicator's vertical distribution to a tide level (e.g., MTL - mean tide level), and the indicative range, which is the possible elevational range occupied by the indicator (e.g., MHHW-MLLW - mean higher high water - mean lower low water). When bio-, litho- or chemo-

stratigraphic data indicates formation within terrestrial or marine conditions, the indicator is classified as a limiting point, which provide an upper or lower limit on RSL, respectively. We summarize the different indicators, their indicative meaning, and evidence used to support our interpretation in Table 1.

3.1.1. Isolation basins

Isolation basins are one of the most precise sea-level indicators in uplifting areas. They comprise a significant part of the database (n = 70 index points, n = 94 terrestrial limiting points). Isolation basins are former topographic depressions that were initially beneath sea level, but which transitioned into freshwater lakes upon isolation from the sea following land uplift. Lithologic and diatom analyses across the marine to lacustrine transitional facies in sediment cores from these environments identify the isolation transition (Corner et al., 1999), which can be dated to provide a chronology for its timing. The isolation contact is generally considered to represent the time when the sill isolating the lake from the sea rises to mean high tide level (Corner et al., 1999, 2001). However, for many basins, a meromictic (salinity stratified) phase develops and persists for some time after isolation (Corner and Haugane, 1993). Moreover, the transition to freshwater conditions depends on streams or surface runoff flowing into the basin. Therefore, the indicative range for the isolation contact is considered to represent mean low water spring tide (MLWS) to mean high water spring tide (MHWS) to account for this possible variability. Unlike other indicators, RSL is measured from the elevation of the isolation basin sill, rather than the elevation of the dated contact, relative to contemporary mean sea level (MSL). Terrestrial limiting points from isolation basins are generally derived from gyttja or peat layers above the isolation contact, indicating times after the lake became separated from the sea.

3.1.2. Raised beaches

Raised beaches (n = 226) are mainly found in Franz-Josef Land and Novaya Zemlya, where they form in several levels marking the gradual lowering of RSL. Beaches and coastal bars usually form above mean tide level due to wave accumulation of coarse material (sand, gravel, pebble). Modern beach elevation can vary, forming at lower elevations in closed gulfs and bays and higher elevations in areas exposed to direct storm fetch (Forman et al., 2004); therefore, we conservatively applied an indicative range from mean lower low water (MLLW) to 3 m above the highest astronomical tide (HAT). On raised beaches, driftwood, allochtonous peat or marine mammal bones can be dated, giving evidence of the beach's age. Beach sediments in outcrops can also be dated using OSL (optical stimulated luminescence) or GSL (green stimulated luminescence).

3.1.3. Erratic blocks on top of a marine terrace

Two index points were obtained using ^{10}Be dating of erratic blocks on the surface of raised marine terraces from the White Sea. The specific palaeogeographic postglacial conditions of the White Sea permitted their use as sea-level indicators (Baranskaya and Romanenko, 2017). At the LGM, when the territory was under the ice sheet, flows at its base plucked and displaced large gneiss blocks from under the glacier. Immediately after its retreat, water filled the White Sea basin, covering the erratic blocks. As GIA uplift caused the coast to rise above sea level, accumulation of the ^{10}Be signal in the gneiss blocks began. Exposure dating of the top surface of the blocks enabled estimation of the time they rose above sea level. ^{10}Be starts accumulating as soon as the rock is first exposed above water, although the impact can be diminished during high tides when the rock is covered; therefore, we estimated the indicative meaning as lowest astronomical tide (LAT) to mean high water (MHW).

3.1.4. Marine terraces

Two index points from raised marine terraces were obtained from coasts of the White and Laptev Seas. Marine terraces can be both accumulative and erosional and form under relatively calm

Table 1
Criteria used to estimate indicative meanings of the samples in the Russian Arctic database.

Sample Type	Evidence	Reference Water Level	Indicative Range
Isolation basin (index point)	Gyttja or gyttja mud with diatom assemblages containing both freshwater and salt water species; changes in lamination and (or) sediment composition	(MLWS + MHWS)/2	MHWS-MLWS
Isolation basin (terrestrial limiting)	Freshwater peat or gyttja overlaying marine sediments	MHWS	>MHWS
Raised beach or coastal bar	Raised beach or coastal bar expressed in the topography	(MLLW + HAT+3 m)/2	(HAT+3m)-MLLW
Driftwood, allochtonous peat or marine mammal bones on raised beaches or inside the sediments of a marine terrace	Driftwood, allochtonous peat or marine mammal bones on the surface of a raised beach, distinct in the topography or inside the body of a terrace composed by marine sediments	(MLLW + HAT+3 m)/2	(HAT+3m)-MLLW
Beach sediments	Beach or tidal sediments	(MLLW + HAT+3 m)/2	(HAT+3m)-MLLW
Erratic blocks on top of a marine terrace	Glacier-deposited blocks of rock on the surface of a raised marine terrace composed by sediments of marine origin	(LAT + MHW)/2	MHW-LAT
Marine terrace	Marine terrace expressed in the topography	(MLWS + MHWS)/2	MHWS-MLWS
Salt marsh (laida)	Salt marsh plant macrofossils or laida sediment textures; geomorphologic evidence (low surface inundated during storm surges)	(MLWS + MHWS + 2 m)/2	MHWS+2m)-MLWS
Deltaic salt marsh	Deltaic sediments: peat above clayey or silty deposits with salt water microfossils	(MLWS + MHWS + 2 m)/2	MHWS+2m)-MLWS
Marine limiting (deltaic sediments)	Layers of sand and silt interbedded with allochtonous peat and grass debris, presumably accumulating on the underwater slope of a marine delta	MTL	<MTL
Transgressive contact	Terrestrial sediments overlain by marine sediments containing marine fauna	(MLWS + MHWS)/2	MHWS-MLWS
Marine limiting	Identifiable in-situ marine shells, calcareous foraminiferal assemblages, prevalent salt water diatoms or high marine salt content in clastic sediment	MTL	<MTL
Terrestrial limiting	Freshwater peat; sediments of terrestrial origin: alluvial, boggy, lacustrine, aeolian,; dated artefacts from ancient human settlements	MTL	>MTL

wave conditions that create their flat surface (Kaplin and Selivanov, 1999). We estimated an indicative range for marine terraces of MLWS-MHWS. There is limited availability of material to precisely date these features. For example, in many of the original studies, marine terraces in an elevation range are attributed to a certain age, but no radiometric age is provided. Due to this lack of precision, 29 points of this type were excluded from the database.

3.1.5. Laidas

Six index points come from laidas. The term "laida" is a local name for environments analogous to temperate salt marshes in Western and Eastern Siberia. These are low surfaces (up to 3 m above sea level) inundated during the highest tides and storm surges. They are usually composed of interbedded peat and clastic sediments. Therefore, peat or occasionally wood are often used to date these features. Laidas are encountered at Yamal and Gydan Peninsulas (West Siberian platform) and on the coasts of the Laptev Sea. Their indicative range is MLWS to 2 m above MHWS, to account for the possible action of storm surges raising the water surface above tide level.

3.1.6. Deltaic salt marshes

64 index points in the database come from prograding Holocene deltas, such as the Northern Dvina Delta (Zaretskaya et al., 2011). Such low deltaic surfaces are composed of interbedded peat, sand, and mud. Their lithologic composition is similar to laidas; however, the topography is different as they usually form numerous islands dissected by river channels. The salinity preference of diatoms contained in salt marsh peats and deltaic muds are used to classify samples as index points (due to the presence of brackish diatoms) or terrestrial limiting (based on freshwater diatoms). Because low deltaic surfaces can be inundated during the highest tides and storm surges, we infer their indicative range to be MLWS to 2 m above MHWS.

A large number of data (n = 77) comes from organic-rich layered deposits of the Lena Delta's first terrace composed of interbedded sediments and plant debris – the so-called "sloyonka" (Bolshiyanov et al., 2013; Makarov, 2009). These sediments formed in a large basin experiencing short-term water-level fluctuations, indicative of a shallow estuary of the paleo-Lena River. Because of the presence of syngenetic ice, Makarov (2009) infers that the deposits accumulated in very shallow conditions, where the ice could freeze to the bottom in winter, and therefore interprets these sediments as index points. However, to be conservative, we assume the deposits are marine limiting because the exact depth of the paleo-delta is unknown.

3.1.7. Transgressive contacts in bottom columns of marine sediments or on land

19 index points are from transgressive contacts found primarily in columns of marine bottom sediments. The timing of transition is derived from dating layers between freshwater and marine sediments. Transgressive contacts can also be found on land, where terrestrial sediments can be overlain by marine facies (e.g., peat lying under marine sand on raised beaches; Bolshiyanov et al., 2009). Their indicative range is MLWS-MHWS.

3.1.8. Terrestrial and marine limiting indicators

Terrestrial limiting data (n = 80) are derived from layers of autochthonous freshwater peat, as well as alluvial, lacustrine, boggy, aeolian and other types of continental deposits. Support for deposition within these environments is provided by the presence of freshwater diatom complexes and other freshwater microfossils. Marine limiting data (n = 69) is provided by in-situ marine mollusc shells, bottom sediments containing marine diatoms and foraminifera, and chemical properties of sediments.

3.2. Ages of sea-level indicators and their uncertainty

The age measurements of samples from the database were made using ^{14}C, Uranium-series, optically stimulated luminescence (OSL), infrared stimulated luminescence (IRSL), green stimulated luminescence (GSL) electron spin resonance (ESR), or ^{10}Be.

Most samples (n = 596) were radiocarbon (^{14}C) dated using both AMS and conventional methods. Given the age of studies used in the database, some published dates were not previously corrected for isotopic fractionation. For these samples, we accounted for isotopic fractionation of δ^{13}C values (wood or peat: $-23 > \delta^{13}C > 31‰$; marine carbonates: $4 > \delta^{13}C > 4‰$ (Stuiver and Polach, 1977); using a 4‰ (~64 ^{14}C yr) δ^{13}C uncertainty term. If it was unknown whether a sample was initially corrected for isotopic fractionation in the original study, the sample was not corrected, but an uncertainty equal to the sum of the possible age correction and its uncertainty was applied.

Approximately two thirds of the ^{14}C-dated samples came from bulk sediment or peat samples that may have incorporated contaminating sources of older (e.g., dissolved CO_2 or HCO_3 from thawing older permafrost) or younger (e.g., contemporary plant roots penetrating older sequences beneath the sediment surface) carbon. A ±100 ^{14}C yr error was applied to bulk samples to account for sample contamination (Törnqvist et al., 2015). The total ^{14}C uncertainty was calculated as the quadratic sum of analytical (measurement), bulk, and isotopic fractionation uncertainties (Törnqvist et al., 2015).

Using the recalculated ^{14}C age and its uncertainty, all ^{14}C dates were recalibrated using the IntCal13 and Marine13 calibration curves (Reimer et al., 2013) for terrestrial and marine carbonates, respectively. To account for the local marine reservoir effect, in the case where its values were not reported by the original study, reservoir correction (ΔR) values and uncertainties from the Marine Reservoir Correction database (http://calib.qub.ac.uk/marine/) were applied. Calendar ages are given in calibrated years before present, where present is considered as the year 1950 AD.

29 samples were dated using the OSL method. The single aliquot regenerative dose protocol applied to quartz grains was used to estimate the equivalent dose (Murray and Wintle, 2000). The samples were analyzed for natural series radionuclide concentrations in the laboratory, using high-resolution gamma spectrometry (Murray et al., 1987). These concentrations were converted into dose rates using the conversion factors listed by Olley et al. (1996). The ages were not corrected for sample burial depth.

Four samples in the database were obtained from shells of molluscs dated using the U-series method. As the measured activity ratios were not reported, we were unable to recalculate the ages; therefore, the dates are provided as reported by the original studies (Bolshiyanov et al., 2009).

Five samples from the core from Lake Changeable on Severnaya Zemlya (Raab et al., 2003) were dated using infrared-stimulated luminescence (IRSL), multi-aliquot dating (e.g., Aitken, 1998) conducted on the polymineral fine-silt fraction.

Two samples were dated using the GSL method. They were both excluded from further analysis as the authors (Møller et al., 2006) suppose that the dated material (shell and marine clays) were displaced.

Two shells of marine molluscs were dated using the electron spin resonance (ESR) method. The technique is based on the premise that certain crystals behave as natural dosimeters. This means that electrons and holes had accumulated over time in the crystal lattice induced by surrounding radiation. The age was

obtained by calculating the dose received compared to the dose rate generated by the surrounding environment, mainly radioisotopes K, U, and Th. One of these samples was excluded from further analysis because the information concerning the sample was insufficient.

Two samples were dated using the ^{10}Be method, one of the methods of exposure dating using cosmogenic nuclides. They were taken from the upper 2 cm of gneiss erratic blocks standing on the surface of raised marine terraces. Exposure ages were computed from the measured blank-corrected concentrations of ^{10} Be and the local production rate in quartz (Young et al., 2013), taking into account the thickness of the sample, its density, and the shielding of the sampling site by surrounding topography and snow in winter.

3.3. Estimation of RSL and its uncertainty

RSL recorded by each sample was calculated using the following equation:

$$RSL_i = A_i - RWL_i,$$

Where A_i and RWL_i are the altitude and the reference water level of sample i, which are both expressed relative to MSL and are characterized by uncertainties determined by many factors. Uncertainties of the vertical RSL position can generally be divided into three sources: 1) measurements of the sample depth in a core or section; 2) measurement of elevation of the top of the borehole or section relative to MSL; and 3) determination of the sample's indicative meaning and possible errors in its estimation. For each of the groups, all possible sources of uncertainties were quantitatively evaluated and are listed in Table 2.

For all samples, save isolation basins, uncertainties in determining the sample depth in a core or a section can significantly affect the vertical RSL position in the past. Therefore, for each sample, a detailed description of the core or section was produced, including dated facies, dated material, overburden and underlying facies, depth of sample in the section or borehole and depth to consolidated substrate. Sedimentary samples were classified as basal or intercalated, to account for their possible compaction, and their sample thickness was indicated. However, most of the samples from the Russian Arctic database are from non-sedimentary units, which do not experience significant compaction.

Uncertainties in the absolute elevation measurement differ significantly from method to method (Table 2). If possible, an elevation was referenced to an orthometric datum, which in Russia is the Baltic system of heights. If this was not possible, the samples were related to MSL. As local MSL changes through time, an analysis of its possible variations was made according to tide gauge data across the Russian Arctic. The observed sea-level change trends in the White, Barents, Kara and Laptev Seas did not exceed 0.5 cm/yr (Proshutinsky et al., 2004), making no more than 0.25 m in 50 years when the elevations were measured. Therefore a benchmark uncertainty of 0.25 m was added for samples referenced to MSL to account for its temporal changes. The epoch in which the sample was related to MSL was also recorded.

An additional uncertainty was added to account for the possible difference in MSL and 0 elevation of the Baltic system of heights. According to the data by the Arctic and Antractic Research Institute system ESIMO (http://portal.esimo.ru/portal/esimo-user/data;jsessionid=9A2B0D9475E1D26D7CD08B710D702621), the station datums related to the Baltic System are provided along with MSL average long-term values. Based on data with the longest open-access continuous datasets available (34 tide gauges across the Barents, White, Laptev and Kara Seas basins), we estimated this uncertainty as 0.9 m, to account for the possible difference between the local MSL and the Baltic system.

For the estimation of the indicative meanings, numerical values of relevant tidal datums were estimated using the closest tide gauge to the sampling point. If a point was situated at an equal distance between several tide gauges, average values were taken.

4. Results

The database consists of 385 index points, 149 marine limiting dates, and 90 terrestrial limiting dates. Data is concentrated in the more easily accessed European part of Russia, and is relatively sparse in formerly non-glaciated regions. The database spans the LGM to present, although for some areas, large temporal gaps exist (Figs. 4–6).

4.1. Baltic shield (Regions 1–11)

4.1.1. Northern Kola Peninsula (Regions 1–3)

The record from the northern Kola Peninsula consists of 26 index points (20 from isolation basins, three from driftwood on raised coastal bars, one from a marine terrace and two from raised

Table 2
Fields related to vertical position of RSL.

Uncertainties related to vertical position of RSL (elevation)	Explanation
Uncertainties in determining the depth of a sample in a core or section	
Sample thickness uncertainty	Uncertainty related to the thickness of the dated sample; 1/2 of the sample thickness.
Sampling uncertainty	Uncertainty related to measuring the depth of a dated sample within a core or section; ± 0.01 m
Core shortening/stretching uncertainty	Uncertainty related to compaction during coring; ± 0.15 m for rotary coring and vibracoring, ± 0.05 m for hand coring and ±0.01 m for a Russian sampler
Non-vertical drilling uncertainty	Uncertainty related to non-vertical coring; 0.02 m/m depth
Uncertainties in determining the absolute elevation of a core, sample or section	
Tidal uncertainty	Applies only to samples collected offshore with reference to the water surface; ½ of the tidal range (Shennan, 1989)
Water depth uncertainty	For water depths measured offshore using fathometers, echo sounders, etc.; ±0.5 m (Hijma et al., 2015)
Leveling uncertainty	±0.03 m if the leveling method is unknown (Törnqvist et al., 2004)
GPS uncertainty	±0.1 m for the accuracy of GPS measurements (Hijma et al., 2015)
Benchmark uncertainty	±0.1 m for uncertainties in benchmark elevations (Engelhart, 2010); ±0.25 m for samples related to MSL
Map uncertainty	1/2 the contour line interval for elevations measured on topographic maps
Uncertainty for the discrepancy between MSL and 0 elevation of the national datum (Baltic system of heights)	±0.9 m, derived from 1/2 of the absolute value of the maximum difference between local MSL and the Baltic system of heights at 34 tide gauges across the Barents, White, Laptev and Kara Seas basins
Uncertainties associated with the sample's indicative meaning	
Indicative range uncertainty	1/2 of the indicative range (as the indicator can occupy any part of it in the contemporary environment)

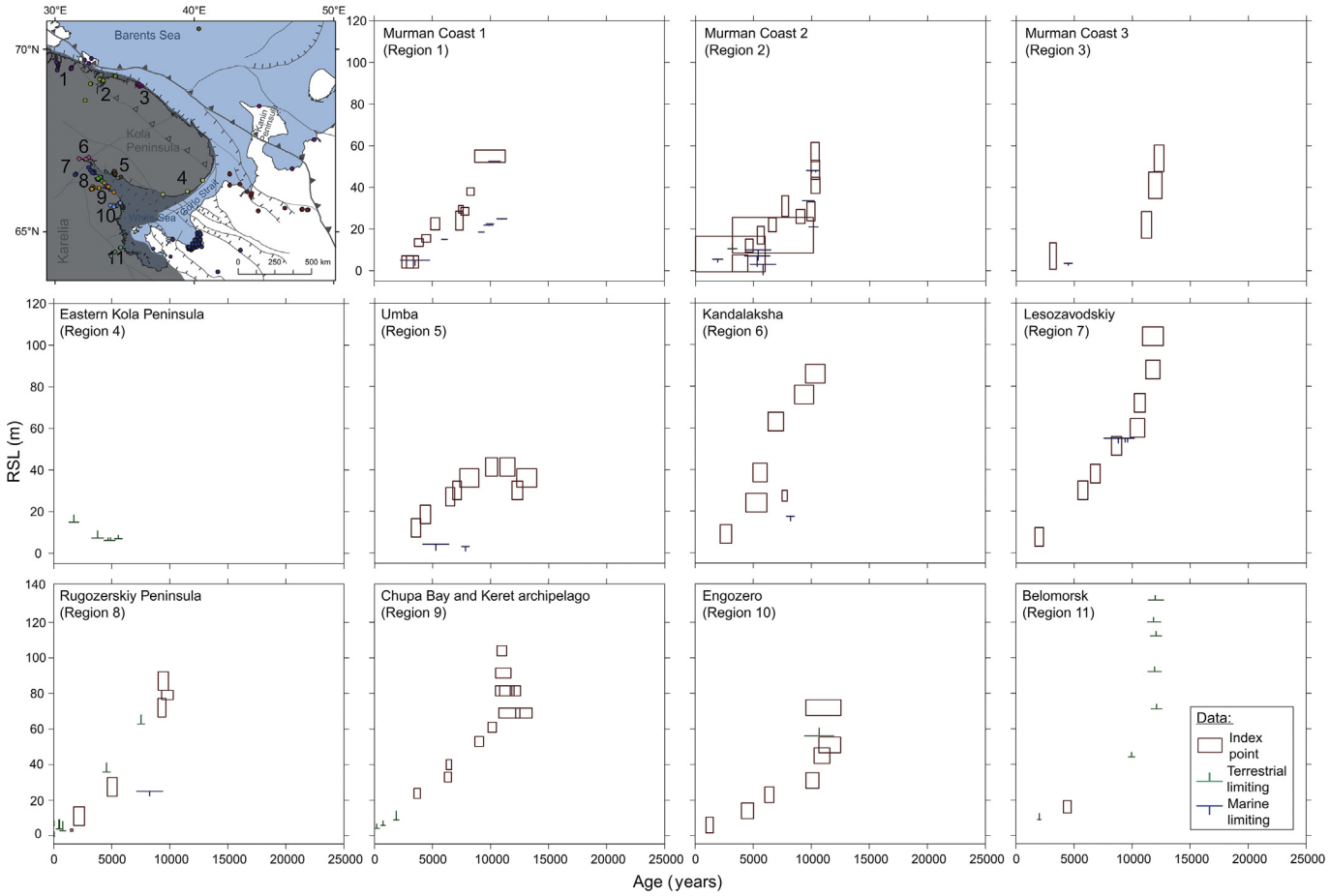

Fig. 4. RSL data for the Baltic Shield.

beaches), one terrestrial limiting point and 16 marine limiting points from shells of marine molluscs (Fig. 4).

On the Murman coast of the Kola Peninsula, the upper marine limit of raised beaches reaches 80–100 m (Baranskaya, 2015; Koshechkin, 1979). However, the highest dated isolation basins are situated less than 60 m above modern sea level. The records show a pattern of RSL fall, slowing down from the LGM to present. The amplitudes of the RSL fall generally decrease from west to east. In the westernmost part, close to the Russian-Norwegian border (Region 1, Murman Coast 1), RSL fell from 55.0 ± 2.9 m at 10.1 ka to 33.0 ± 5.0 m at 7.5–8.3 ka and finally to 13.5 ± 1.8 m at 3.8 ka (Corner et al., 1999). To the east (Region 2, Murman Coast 2), RSL decreased from 57.0 ± 4.5 m at 10.3 ka to 12.0 ± 3.1 m at 4.6 ka (Corner et al., 2001). Further eastwards (Region 3, Murman Coast 3), data from isolation basins capture the time immediately after deglaciation; RSL dramatically fell more than 30 m in ~1 kyr from 54.0 ± 6.3 m at 12.3 ka to 22.0 ± 6.3 m at 11.0 ka (Snyder et al., 1997). After a gap in data in the mid Holocene, an index point from an isolation basin shows RSL of 7.0 ± 6.3 m at 3.2 ka.

4.1.2. White Sea coasts (Regions 4–11)

For the western White Sea coasts, 50 index points from isolation basins (n = 46), erratic blocks on marine terraces (n = 2), and driftwood (n = 2), 23 terrestrial limiting, and nine marine limiting points provide continuous regional records of RSL fall, although a possible highstand in the early postglacial time is shown in Regions 5 and 9 (Fig. 4). Amplitudes of RSL fall generally increase towards the apex of Kandalaksha Gulf.

On the Eastern Kola Peninsula (Region 4), the Holocene marine limit is seen up to 7–10 m as a series of uplifted beaches and coastal barriers, indicating a slight Holocene RSL fall – the smallest on Baltic shield. However, only terrestrial limiting archaeological remnants were dated, placing the upper sea-level limit at 6.2 ± 1.0 m at 4.6–5.5 ka (Koshechkin, 1979).

The southern coast of Kola Peninsula near Umba settlement (Region 5) is characterized by a record of isolation basins extending into the Younger Dryas (Kolka et al., 2013a). Marine facies overlying clays of a freshwater postglacial basin (the "White Sea proglacial lake" as per Patton et al., 2017) show gradual RSL increase from 30.0 to 36.0 m at 12.4–13.0 ka to 41.3 ± 4.4 m at 11.5 ka, followed by a highstand persisting ~1 kyr. After that, RSL fell from 41.3 ± 4.4 m at 10.1 ka to 12.0 ± 4.4 m at 3.5 ka.

Kandalaksha (Region 6), Lesozavodskiy (Region 7) and Rugozerskiy Peninsula (Region 8) provide the highest dated coastlines in the Russian Arctic of up to 100 m. Isolation basin data only span the Holocene and show rapid RSL fall at the beginning of the Holocene that decays exponentially. At Kandalaksha (Region 6), RSL lowers from 86.0 ± 4.4 m at 10.3 ka to 9.0 ± 4.4 m at 2.6 ka (Kolka and Korsakova, 2010). At Lesozavodskiy (Region 7), lakes at 104.0 ± 4.4 and 88.0 ± 4.4 m were isolated at 11.8 and 11.6 ka, respectively, while at the end of the Holocene, RSL was at 7.6 ± 4.4 m at 2.0 ka (Kolka et al., 2005). Isolation basin data from Rugozerskiy Peninsula (Region 8) indicate higher RSL position than Kandalaksha and Lesozavodskiy, making Rugozerskiy Peninsula the fastest uplifting area in the Russian Arctic. RSL was at 87.0 ± 5.2 m at 9.3 ka exponentially lowering to 11.0 ± 5.2 m at 2.1 ka (Romanenko

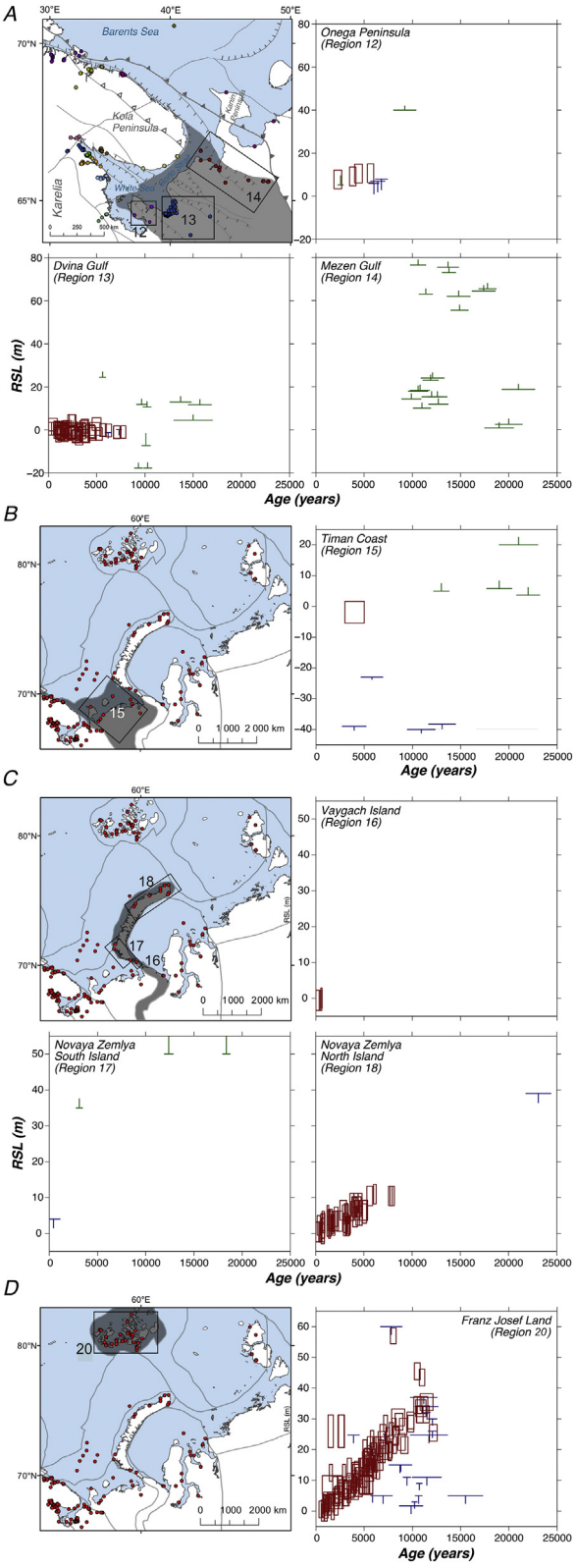

Fig. 5. RSL data for the European Russian Arctic: A) Russian Plate, B) Timan-Pechora Plate, C) Novaya Zemlya fold belt, D) Franz-Josef Land.

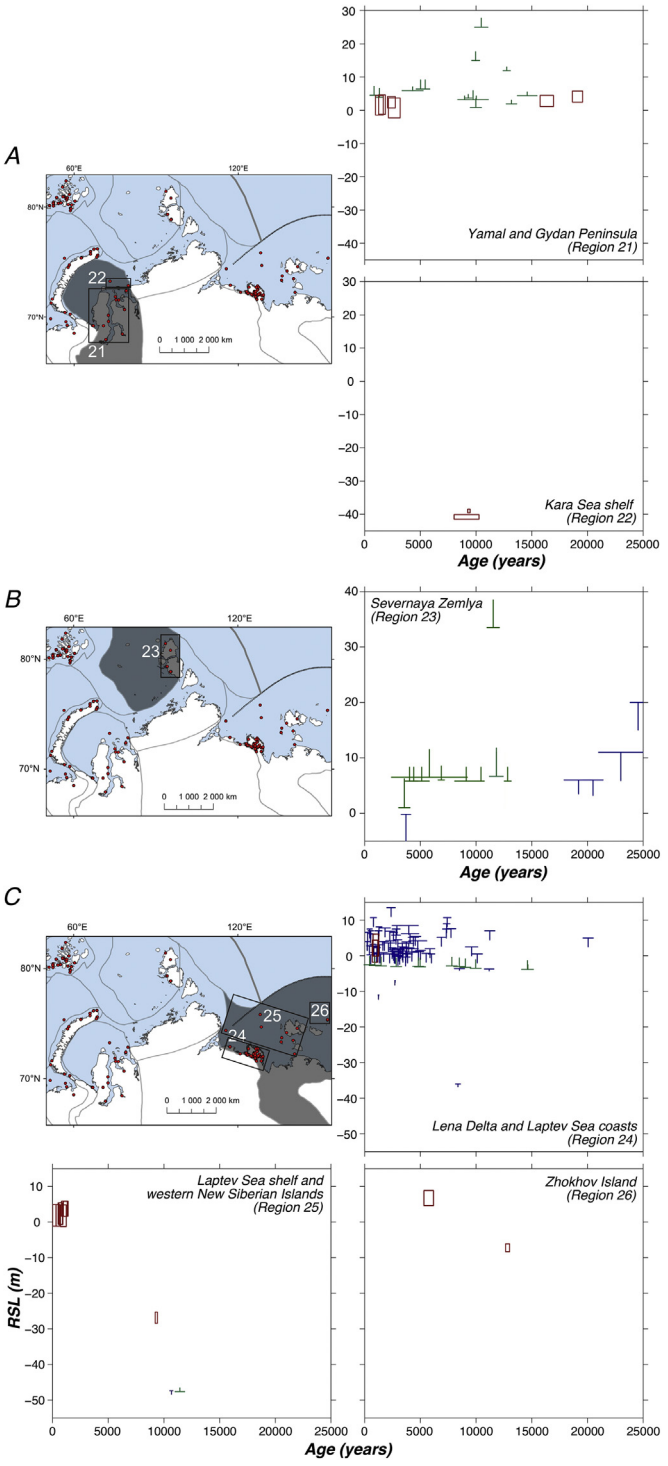

Fig. 6. RSL data for the Siberian Russian Arctic: A) West Siberian Basin, B) Severnaya Zemlya, C) - Laptev Sea continental margin.

and Shilova, 2012).

The RSL history of Chupa Bay and Keret archipelago (Region 9) extends into the Younger Dryas and is constrained by 11 index points (Kolka et al., 2015) and three terrestrial limiting points (Baranskaya and Romanenko, 2017) from isolation basins. As in Umba (Region 5) situated opposite to Chupa Bay and Keret archipelago (Region 9) on the coast of the Kandalaksha Gulf, early postglacial sea-level rise is documented: marine sediments with

saltwater diatom assemblages overlie varved clays of the proglacial freshwater basin. Dates from the transitional facies in marine sediments suggest rapid transgression from 69.0 ± 2.7 m at 12.9 ka to 81.5 ± 2.7 m at 12.3 ka, followed by a highstand in RSL of ~104 m persisting ~1.2 kyr, indicated by an anomalously thick gyttja layer with brackish diatoms in an isolation basin (Kolka et al., 2015). Following the highstand, RSL fell from 81.5 ± 2.7 m at 11.1 ka to 61.0 ± 2.7 m at 10.1 ka. RSL continued to fall in the mid-Holocene and reached 24.0 ± 2.7 m at 3.6 ka.

At Engozero (Region 10), RSL fall is reconstructed from eight isolation basins (Kolka et al., 2013b), with slight scatter in post-isolation contacts at the beginning of the Holocene. RSL fell rapidly from 72.0 ± 4.4 to 45.0 ± 4.4 m between 11.5 and 10.6 ka to 31.0 ± 4.4 m at 10.1 ka and continued to fall at a slower rate from 14.0 ± 4.4 m at 4.5 ka to present.

In Belomorsk (Region 11), the Early Holocene record consists of terrestrial limiting isolation basin data by Lunkka et al. (2012) that reflects simultaneous separation of five lacustrine depressions at 72.0 ± 2.5 to 130 ± 2.5 m above modern sea-level from a larger freshwater body (the White Sea proglacial lake) at 11.9–12.1 ka without any penetration of marine water, implying RSL lower than 72.0 ± 2.5 m at 12.0 ka. A terrestrial limiting date from an isolation basin indicates RSL was below 44.0 ± 2.5 m by 9.9 ka. An index point from driftwood in beach facies places RSL at 15.8 ± 3.4 m at 4.5 ka and one terrestrial limiting point from dated coal in a Neolithic settlement constraints it at less than 9 ± 2.5 m at 2 ka.

4.2. Russian Plate (Regions 12–14)

The RSL history of the Russian Plate is constrained by 115 points characterized by uneven spatial distribution (Fig. 5A). The south-west of the area is relatively well studied and covered by a dense network of points, while in the northeastern portion, there are evident data gaps.

4.2.1. Onega Peninsula (Region 12)

Southern Onega Peninsula (Region 12) is characterized by four index points, two terrestrial limiting and three marine limiting points. They show RSL below 40.0 ± 1.0 m at 9.4 ka and above 8.0 ± 5 m at 6.4 ka, as suggested from one terrestrial limiting point from peat (Koshechkin, 1979) and three marine limiting points from sediments of an ancient lagoon (Boyarskaya et al., 1986). Index points from isolation basins (Repkina et al., 2018) indicate RSL fall since the mid-Holocene from 10.7 ± 4.3 m at 5.7 ka to 7.8 ± 4.3 m at 2.1 ka.

4.2.2. Dvina Gulf (Region 13)

The RSL history of the Dvina Gulf coasts is described by abundant data (67 index points, 35 terrestrial limiting and four marine limiting dates) from deltaic peaty sediments. Early Holocene data place an upper limit on RSL of 24.0 ± 2.5 m at 10.2 ka and of 10.0 ± 2.5 m at 9.6 ka. Two terrestrial limiting dates from freshwater peat limit RSL to below −17.7 ± 0.4 m between 9.3 and 10.2 ka (Koshechkin, 1979), suggesting an Early Holocene lowstand. Slight RSL rise is documented from −2.9 ± 2.9 m at 5.7 ka and −3.9 ± 2.9 m at 3.8 ka to 0.9 ± 2.9 m at 1.9 ka (Zaretskaya et al., 2011).

4.2.3. Mezen Gulf (Region 14)

Data from the Mezen Gulf are restricted to 20 terrestrial limiting points from OSL-dated fluvial and glaciofluvial sands (Larsen et al., 2006). They indicate RSL was below modern between 19.0 and 20.0 ka, and below 10–14 m between 9.9 and 11.0 ka.

4.3. Timan fold belt and Timan-Pechora Platform (Timan Coast, Region 15)

The RSL history of the Timan coast is constrained by nine points (Fig. 5B). Data from a marine sediment column show RSL above −38.7 ± 1.6 m at 11.3 ka (Krapivner, 2006). Marine limiting dates from shells (Polyak et al., 2000; Zhuravlev et al., 2013) place RSL above −40.0 ± 1.5 m at 10.9 ka and −23.0 ± 1.2 m at 5.7 ka. Terrestrial limiting dates from OSL-dated fluvial, lacustrine and aeolian sands (Larsen et al., 2006) indicate RSL lower than 6.0 ± 2.7 m from 22 to 13 ka. An index point from beach sand indicates that RSL rose from −1.8 ± 3.7 m at 4 ka to present level.

4.4. Ural-Novaya Zemlya fold belt (Regions 16–18)

The Ural-Novaya Zemlya fold belt is characterized by 62 points grouped into three regions: Vaygach Island (Region 16), the South (Region 17) and the North Island of Novaya Zemlya archipelago (Region 18) (Fig. 5C).

The record of Vaygach Island (Region 16) is limited to the last 0.6 ka. Index points from three dated logs on raised beaches show little RSL change to present within their uncertainties.

On the South Island of Novaya Zemlya (Region 17), freshwater peat place an upper limit on RSL of 35 ± 2.7 to 50 ± 5.1 m from 18 to 3 ka (Bolshiyanov et al., 2006; Zhuravlev et al., 2013). A *Mytilus edulis* shell places RSL above 4.0 ± 2.5 m after 0.6 ka, indicating an ongoing RSL regression.

The North Island (Region 18) has the most complete record. One marine limiting date from a marine mollusc shell suggests RSL was above 39 ± 2.7 m at 23 ka (Bolshiyanov et al., 2009). There is a gap in the record until 8.0 ka. 54 index points from driftwood or bones of marine mammals on raised beaches (Forman et al., 2004) show stable RSL of 10.4 ± 2.9 m from 7.9 to 6.1 ka. RSL then fell from 10.4 ± 2.9 m at 5.6 ka to 2.2 ± 2.9 m at 1.9 ka.

4.5. Barents Sea shelf (Region 19)

Due to considerable water depths of the Barents shelf (up to 350 m), the only source of sea-level data comes from marine drilling. Eight marine limiting dates from transgressive contacts (Krapivner, 2006) place RSL above −113 ± 3 to −350 ± 1.1 m in the late Glacial period and early Holocene, and above −62 ± 1 m in the late Holocene; however, these data were excluded from further analysis due to the absence of the ^{14}C age uncertainty in the original publication.

4.6. Franz-Josef Land (FJL) (Region 20)

The RSL history of FJL is constrained by 22 marine limiting points from marine mollusc shells and 149 index points from driftwood and marine mammal bones on raised beaches (Fig. 5D). The data show continuous RSL fall during the whole Holocene, from 47.0 ± 2.9 m at 11 ka to 15.0 ± 2.9 m at 5 ka and to 5.0 ± 2.9 m at 2.5 ka; it forms a relatively smooth curve with higher scatter at the beginning of the Holocene. However, there are several outliers in this relatively uniform history.

4.7. West-Siberian Platform (Regions 21, 22)

There is relatively little RSL data available for the West Siberian Platform (n = 26) (Fig. 6A). The Yamal and Gydan Peninsula (Region 21) record consists of 9 index points from laidas (Romanenko et al., 2015) and deltaic salt marshes (Makeev, 1988) and 15 terrestrial limiting dates from freshwater peat (Grigorieva, 1987; Gusev et al., 2013b; Makeev, 1988, etc.). RSL was near the present level during

deglaciation: 4.2 ± 1.7 m at 19.0 ka and 2.9 ± 1.7 m at 16.0 ka (Grigorieva, 1987). In the middle-late Holocene, terrestrial limiting data suggest RSL was no higher than 0.9 ± 2.7 m between 15.0 and 9.0 ka, and no higher than 6.0 ± 1.1 m between 4.3 and 5.4 ka. Laida peat indicates RSL at 0.8 ± 2.9 m at 2.6 ka and suggests a small highstand of 2.5 ± 1.7 m at 2.4 ka is possible.

The Kara Sea shelf (Region 22) record consists of two marine limiting points from shells at transgressive contacts from marine sediment columns. They place RSL above −40.8 ± 1.2 m at 9.1 ka (Levitan et al., 2007) and above −39.0 ± 1.1 m at 9.3 ka (Polyakova and Stein, 2004) in different locations.

4.8. Severnaya Zemlya (Region 23)

RSL data from Severnaya Zemlya is also not abundant (n = 16), including 1 index point, 5 marine limiting and 10 terrestrial limiting dates (Fig. 6B). Most of them are derived from the Lake Changeable isolation basin (Bolshiyanov and Makeev, 1995; Raab et al., 2003); other data come from shells of marine molluscs, alluvial, alluvial-marine and boggy sediments (Bolshiyanov and Makeev, 1995).

Shells found on marine terraces suggest RSL was above 20.0 ± 5.0 m at 24.5 ka and above 11.0 ± 5.1 at 23 ka (Bolshiyanov and Makeev, 1995); IRSL-dated feldspar fine-silt fraction from the core of Lake Changeable place it above 6.0 ± 2.8 m between 20.5 and 19.2 ka (Raab et al., 2003). Terrestrial limiting ^{14}C dates from humic acids in the bottom column of Lake Changeable (Raab et al., 2003) and from willow fragments in outcrops near this lake (Bolshiyanov and Makeev, 1995) suggest RSL below 6.0 ± 2.8 m from 12.8 till 4.0 ka and below 6.5 ± 5.0 m at 11.7 ka and 3.4 ka, respectively. A marine limiting date from plant debris in alluvial-marine sediments (underwater part of a local delta) (Bolshiyanov and Makeev, 1995) places RSL above −0.2 ± 5.5 m at 3.7 ka.

4.9. Laptev Sea continental margin (Regions 24–26)

The RSL record for the Laptev continental margin consists of 111 points (85 marine limiting points, 14 index points and 12 terrestrial limiting points, Fig. 6C).

4.9.1. Lena Delta and Laptev Sea coasts (Region 24)

The record for Lena Delta and the Laptev Sea coasts includes 97 data points, including two index points from driftwood on raised beaches (Bolshiyanov et al., 2013), 84 marine data from organic-rich, shallow marine or deltaic sediments of the Lena Delta (n = 79) (Bolshiyanov et al., 2013; Makarov, 2009) and shells and plant remains above transgressive contacts (n = 5) (Winterfeld et al., 2011) and 11 terrestrial limiting dates from plant debris in lacustrine and aeolian sands in Nikolay Lake bottom sediments (Andreev et al., 2004). The RSL record from this region contains a great deal of scatter with terrestrial and marine limiting dates contradicting each other. RSL fell from above 5 ± 2.7 m at 20.0 ka to below −3.9 ± 2.5 m at 14.7 ka. The Holocene RSL behavior is not well constrained, although RSL reached 3.0 ± 3.2 m at 0.9 ka.

4.9.2. Laptev Sea shelf and Western New Siberian Islands (Region 25)

Ten index points from transgressive contacts (Holmes and Creager, 1974; Polyakova et al., 2005) and raised beaches (Anisimov et al., 2009a; Bolshiyanov et al., 2013), one marine limiting and one terrestrial limiting date from transgressive contacts (Bauch et al., 1999) comprise the Laptev Sea shelf and Western New Siberian Islands RSL history. Index points place RSL at −52.5 ± 1.1 m at 17.1 ka and −41 ± 1.1 m at 12.8 ka. A pairing of terrestrial and marine limiting dates that indicate RSL was ~-47 m between 11.4 and 11.6 ka. RSL rose to −27.0 ± 1.6 m at 9.3 ka. There is a gap in the early to middle Holocene record. Raised beaches suggest RSL fell from 3.7 ± 2.3 m at 1.1 ka to present in the late Holocene.

4.9.3. Zhokhov Island (Region 26)

The Zhokhov Island record is derived from two index points from a raised beach and lagoon deposits (Anisimov et al., 2009b). RSL rose from −7.2 ± 1.1 m at 12.8 ka to a highstand of 6.7 ± 2.3 m at 5.7 ka, a higher RSL position compared to the central Laptev Sea shelf and the western New Siberian Islands.

5. Discussion

5.1. Temporal and spatial variability of RSL

For discussion of spatial and temporal variability of RSL, we clustered the study regions into formerly glaciated areas, covered by LGM ice sheets, intermediate-field areas (as originally defined in Clark et al., 1978) situated around the former ice margins and experiencing the influence of the proglacial forebulge collapse, and far-field areas (Clark et al., 1978), located away from the glaciated territories and experiencing no considerable rebound or subsidence due to unloading.

5.1.1. Formerly glaciated areas (Regions 1–14, 17–20)

In formerly glaciated areas, the patterns of RSL change are diverse. Glacio-isostatic rebound and eustatic sea-level (ESL) rise have opposite signs, and the resulting RSL behavior depends on the difference in their temporally and spatially variable rates (Kaplin and Selivanov, 1999; Lambeck and Chappell, 2001). This difference, in turn, is driven by: a) ice thickness; b) timing of deglaciation (e.g., if the area becomes ice-free simultaneously with a major meltwater pulse, the catastrophic ESL increase might in some cases exceed glacio-isostatic uplift); c) rate of deglaciation; and d) lithosphere and mantle properties dictating the rate of the isostatic response (Peltier et al., 2015). The combinations of these parameters result in three patterns of RSL change in areas of the Russian Arctic that were glaciated at the LGM.

5.1.1.1. Continuous RSL fall (Baltic shield, Franz-Josef Land, Novaya Zemlya). The greatest RSL fall in the Russian Arctic was observed at the Baltic Shield due to its proximity to the center of the Scandinavian Ice Sheet where ice thickness and associated glacio-isostatic rebound was maximal (Clason et al., 2014; Patton et al., 2017). Consequently, areas near the north-western corner of Kandalaksha Gulf of the White Sea (Regions 6–8, Fig. 4) have the highest amplitudes (up to 100 m) and rates of RSL decrease. On the Murman coast of the Kola Peninsula (Regions 1–3, Fig. 4), the amplitude of maximum post-LGM RSL was lower (up to 60 m), implying smaller ice thickness at the LGM. The Murman coast was characterized by fast ice sheet retreat at 13-12 ka (Hughes et al., 2016). Due to this, GIA presumably outweighed postglacial ESL rise, resulting in RSL fall documented in Region 3 at 11–12 ka. The fastest fall happened from ~12 to 7 ka, and then gradually slowed down.

In contrast, data from Franz-Josef Land (Region 20, Fig. 5D) show relatively slow RSL decline between ~13 and 8 ka and a faster fall after 8 ka. Possible explanations of the weaker GIA signal on FJL relative to the Kola Peninsula are: 1) its smaller LGM ice thickness (300–1200 m in FJL compared to 1800–2500 m in Kola Peninsula; Clason et al., 2014; Svendsen et al., 2004); or 2) the longer presence of local glaciers long after the collapse of the Barents-Kara sheet (Hughes et al., 2016).

For Novaya Zemlya (Regions 17, 18, Fig. 5C), records are unavailable before 8 ka. Stable sea-level position from 8 to 6 ka may

result from comparable rates of ESL rise and glacio-isostatic uplift (Forman et al., 2004). Further RSL decrease was caused by slow-down in ESL rise towards present time (Peltier, 1998, 2002; Lambeck et al., 2014), along with persisting glacioisostatic uplift of the coasts (Forman et al., 1999). Smaller amplitudes of RSL fall in Novaya Zemlya (Regions 17, 18) relative to the Murman coast (Regions 1–3) and FJL (Region 20) imply smaller LGM ice thickness in Novaya Zemlya compared to other ice sheet centers of the western Russian Arctic, although modeling data shows ice thickness similar to FJL (Clason et al., 2014). Overall, to provide the constant lowering of RSL observed across these regions, either a very quick (as on the Murman coast), or a relatively late (as on Franz-Josef Land and Novaya Zemlya) final deglaciation was necessary. Similar examples of continuous post-LGM RSL fall have been described in Arctic Canada (Dredge, 1991; Simon et al., 2014) and Western and Eastern Greenland (Long et al., 2011) in central regions of LGM glaciation where the ice was thick and remained stable for a long time.

5.1.1.2. Post-LGM RSL rise, followed by an early Holocene highstand and subsequent RSL fall (White Sea coasts within the Baltic shield). For some regions of the White Sea (Regions 5, 9, 10, 11, Fig. 4), paleogeographic conditions played a role in post-LGM RSL patterns that differ from other regions with active glacio-isostatic uplift. In contrast to the Murman coast, a post-LGM highstand was observed at these sites due to specific patterns of deglaciation driven by White Sea bathymetry.

During deglaciation, the Kandalaksha Gulf depression acted as a topographic constriction that contributed to the stable position of the Eurasian ice sheet margin in the White Sea (Patton et al., 2017). When the Eurasian ice sheet melted at ~13 ka (Hughes et al., 2016), a proglacial "White Sea ice lake" formed. It was dammed at the Gorlo Strait by a prominent 100 km wide, sub-aerially exposed sill (Patton et al., 2017). Sediments of this proglacial lake were described in the lower part of isolation basin cores in Umba (Region 5) and Chupa (Region 9) (Kolka et al., 2013a, 2015), and further to the southeast in Belomorsk (Region 11) (Lunkka et al., 2012).

The time of discharge of the White Sea proglacial lake is debated (Kolka et al., 2013a, 2015; Lunkka et al., 2012; Patton et al., 2017). Evidence from Belomorsk (Region 11, Lunkka et al., 2012) suggests massive discharge at 12 ka causing immediate isolation of five lakes at elevations from 72 to 134 m from a larger freshwater basin; these lakes were never re-connected to sea following isolation. In Umba (Region 5, Kolka et al., 2013a), sediments of the White Sea proglacial lake were replaced by marine sediments at 13 ka, and RSL rose 11 m over 1.7 kyr. In Chupa (Region 9, Kolka et al., 2015), a later and faster RSL rise of ~30 m occurred from 12.2 to 11.0 ka. We suggest that disagreements in the timing of the White Sea ice lake discharge and following transgression are caused by the presence of residual ice in the Kandalaksha Gulf depression, acting as a local dam and causing later discharge in Regions 9, 10 and 11, compared to Region 5. As a result, the onset of the marine transgression depended not on RSL changes, but on the time of the ice dam destruction, after which sea water immediately flowed into the southwestern part of the White Sea. This explains the simultaneous transition from proglacial to marine facies in several lakes at elevations from 91 to 69 m in Regions 9 and 10, and existing scatter in the data by an immediate transition of freshwater to marine conditions without a subaerial stage. The deglacial transgression patterns on the White Sea coasts provide a rare example of when local RSL depends not only on the interplay of GIA and ESL, but also depends on the elevation and evolution of local dams (Gorlo Strait sill and ice masses in the Kandalaksha Gulf depression).

The proglacial lake phase and following transgression were not documented for the apex of Kandalaksha Gulf (Regions 6–8), as the records in this region are limited to the Holocene (Holmes and Creager, 1974; Drachev et al., 2003; Peltier, 2004; Kolka et al., 2005; Kolka and Korsakova, 2010; Romanenko and Shilova, 2012); these sites were referred to regions experiencing constant RSL fall (see 5.1.1.1).

After complete deglaciation, RSL in the south-western White Sea was mainly driven by GIA, similar to Regions 1–3 and other centers of LGM glaciations worldwide (Long et al., 2011; Simon et al., 2014). After 11.5–12 ka, glacio-isostatic uplift in Regions 5, 9 and 10 resulted in RSL fall during the remainder of the Holocene, with variable amplitudes and patterns. Greater RSL fall rates (about 5 m in 1000 years) were observed in Chupa (Region 9), where the Scandinavian ice sheet was thicker (Clason et al., 2014) and retreated later (Hughes et al., 2016), compared to Umba (Region 5) and Engozero (Region 10).

5.1.1.3. Post-LGM or early Holocene RSL fall to a lowstand, and mid-Holocene rise to a highstand with subsequent fall until present. In the northeastern Russian Plain (Regions 12–14), formerly situated under the flanks of the Scandinavian ice sheet, ice cover was thinner than on the Baltic Shield, Franz-Josef Land or Novaya Zemlya (Clason et al., 2014), and persisted for a shorter period between 22 and 14 ka (Hughes et al., 2016). Although there are few constraints on the postglacial and early Holocene RSL history of these regions (Koshechkin, 1979), data from terrestrial peat below sea level in boreholes in Dvina Gulf (Region 13) suggest a lowstand of -17 ± 0.4 m at about 10–9.5 ka (Fig. 5A). A highstand is seen in records of the northwestern Russian Plain, its elevation being higher (10.7 ± 4.3 m) in Region 12 (Fig. 5A) due to its closer proximity to the center of the Scandinavian ice sheet. Similar to other regions located beneath ice margins (Peltier, 1976; Engelhart et al., 2015; Shennan et al., 1995; Woodroffe et al., 2014), this pattern of change can be attributed to initial glacio-isostatic rebound, resulting in an RSL lowstand, followed by mid-Holocene RSL rise to a highstand due to weakening of the GIA signal and ongoing ESL rise. After the highstand, RSL fell to its present position as the result of a decrease in the meltwater input against the background of the ongoing glacio-isostatic uplift.

5.1.2. Intermediate-field areas (Regions 15, 16, 21–23)

In the areas close to the margins of the Eurasian ice sheet, which were ice-free at the LGM, first-order RSL patterns are driven by a combination of subsidence from collapse of the proglacial forebulge associated with the Eurasian ice sheet complex and ESL rise.

Data coverage is spatially and temporally limited in intermediate-field areas, although it does permit rough estimation and comparison of RSL trends. Within the Timan coast (Region 15, Fig. 5B), the presence of beach sand below sea level at 4 ka suggests the absence of a highstand due to subsidence from forebulge collapse. The Kara Sea shelf (Region 22) demonstrates RSL at about −38 to −40 m around 9 ka, which is much lower than RSL at the Laptev shelf (Region 25) at around 9 ka (about −27 m). By analogy with other regions of proglacial forebulge collapse around the Laurentide and Eurasian ice sheets (Engelhart et al., 2011; Engelhart and Horton, 2012; Gehrels et al., 2004; Vink et al., 2007; Roy and Peltier, 2017), it can be inferred that the combined effects of GIA and ESL resulted in continuous RSL rise, the rates of which decrease monotonically through time.

In Yamal and the Gydan Peninsula (Region 21, Fig. 6A) and Severnaya Zemlya (Region 23, Fig. 6B), RSL reveals a different behavior. Between 19.1 and 16.4 ka, laida peat from Yamal and the Gydan Peninsula (Region 21) shows RSL from 1.6 to 2.9 m, and data from Severnaya Zemlya (Region 23) also provides evidence of RSL above 20 m from 25 to 20 ka, followed by post-LGM RSL fall, which would imply local ice cover at the LGM. However, despite older

models showing LGM ice cover (Forsström et al., 2003; Siegert et al., 1999; Zweck and Huybrechts, 2005), abundant geologic evidence (Astakhov and Nazarov, 2010; Astakhov, 2014; Baranskaya et al., 2013, 2018; Forman et al., 2002; Svendsen et al., 2004) and recent ice sheet models (e.g. Clason et al., 2014; Hughes et al., 2016; Patton et al., 2017; Peltier et al., 2015) both suggest the absence of the LGM ice sheet at Yamal Peninsula (Region 21). Therefore, high LGM sea level in the region might be linked to tectonic uplift, although the rates that would account for such an offset would be anomalously fast for such a stable platform area. At Severnaya Zemlya (Region 23), which was not covered by the Eurasian ice sheet (Hughes et al., 2016; Svendsen et al., 2004), local ice caps, however, existed at the LGM (Patton et al., 2017) and are still present today (e.g., Bolshiyanov and Makeev, 1995). Their melting may have resulted in local glacio-isostatic uplift.

The end of the Holocene is marked by a small highstand at both Severnaya Zemlya (Region 23) and Yamal and Gydan Peninsula (Region 21) records. This highstand can indicate possible effects of tectonic uplift, hydro-isostasy, meltwater redistribution in the far field oceans required to preserve the gravitational self-consistency of the GIA process (Mitrovica and Peltier, 1991), rotational feedback (Wu and Peltier, 1984), or GIA due to ongoing ice melting (in the case of Severnaya Zemlya). The mechanisms influencing RSL histories in the Kara Sea region still remain poorly constrained. Improved data coverage may provide important insights about local ice sheet histories and the drivers and patterns of RSL change.

5.1.3. Far-field areas (Regions 24–26)

The Laptev Sea continental margin was several hundred kilometers distant from the Eurasian ice sheet (Patton et al., 2017), therefore, vertical land motion from the forebulge collapse would be minimal during the Holocene. Analogous to far-field regions in the Atlantic and Pacific (e.g., Khan et al., 2017), processes such as hydro-isostasy, perturbations to the Earth's rotation vector or tectonic movements may drive patterns of RSL change in these Arctic regions (e.g., Wu and Peltier, 1984; Milne and Mitrovica, 1998, 2008; Peltier et al., 2015; Peltier et al., 2018).

Regions 24–26 show far-field RSL behavior of continued post-LGM RSL rise, reaching near- or above-present values ~5–7 ka as the ESL signal diminished (Anisimov et al., 2009b). Although the data are too sparse to permit the estimation of accurate rates, variations in the magnitude of RSL rise vary among sites: at ~12 ka, RSL was deeper than −47 m on the Laptev shelf (Region 25), although in Zhokhov Island (Region 26) it was only −7 m. The magnitude of the Holocene highstand also varied across regions from 3.7 ± 2.0 (Zhokhov Island) to as much as 10 ± 2.5 m (Lena Delta, Region 24); however, sparse (e.g., Laptev shelf and Zhokhov Island) or scattered (e.g., Lena Delta) Holocene data hinder meaningful comparisons across regions. Whereas the variation in highstand magnitude may be explained by varying contributions from hydro-isostasy or rotational feedback, the magnitude of variation in early Holocene RSL position across the Lena Delta and Laptev Sea region requires a contribution from tectonic vertical movements (Drachev et al., 2003; Drachev and Shkarubo, 2017; Franke et al., 1998).

5.2. Influence of tectonic vertical movements on RSL histories

Tectonic movements of the Earth's crust may drive patterns and rates of RSL change that cannot be explained by the interplay of ESL and GIA (Horton et al., 2018). In the Russian Arctic, spatially variable tectonic vertical motion may be manifested in RSL records in two ways: 1) global movements of large tectonic provinces, such as the Baltic Shield or Novaya Zemlya fold belt and 2) regional-scale block movements.

Global scale movements of large tectonic provinces are hard to distinguish from the general GIA signal, as they may raise or lower the whole RSL curve of a region without changing its shape (e.g., Nikolaev, 1988; Nikonov, 1977). Such global scale tectonic uplift is typical for the Baltic shield (Regions 1–11, Shipilov et al., 2006; Zykov et al., 2017), enhancing the GIA effect. Global scale tectonic movements also could potentially contribute to smaller RSL fall amplitudes on Novaya Zemlya (Regions 16–18, Fig. 5C) compared to Franz-Josef Land (Region 20, Fig. 5D). While the modeled LGM Barents-Kara ice sheet thickness is comparable in these areas (Clason et al., 2014; Svendsen et al., 2004), the difference in RSL curve elevations (Holocene fall of ~40 m or more on Franz-Josef Land and less than 20 m on Novaya Zemlya) may result from long-term Mesozoic-Cenozoic tectonic uplift of Franz-Josef Land (Bolshiyanov et al., 2009; Gusev et al., 2013a; Stolbov, 2000).

Regional-scale vertical land motion change the amplitudes of RSL curves at separate sites or cause data scatter in large regions. Vertical land motions are generally observed in formerly non-glaciated areas (Nikolaev, 1988; Musatov, 1996), which are not impacted by high rates of GIA-induced RSL change. The relatively high position of RSL on Zhokhov Island (Region 26, Fig. 6C) compared to the Laptev shelf and western New Siberian Islands (Region 25, Fig. 6C) may be related to tectonic uplift of the De Long Massive, a separate tectonic structure with a distinct geodynamic history (Pease et al., 2014, Fig. 3). The difference in the RSL rise rates on the Laptev shelf (Region 25) and at Zhokhov Island (Region 26) due to differential tectonic movements could exceed 3 m/kyr (Anisimov et al., 2009b). However, sparse data in the Eastern Russian Arctic hinders detailed analysis of such movements.

In the Laptev shelf and Lena Delta (Regions 24 and 25, Fig. 6C), regional-scale differential vertical movements of tectonic blocks may create scatter in its RSL record. The active crustal movements along the diffuse border between the North-American and the Eurasian lithospheric plates in the Laptev Sea Rift System (Drachev, 1998; Drachev et al., 2003; see Fig. 3) could potentially change the magnitude of highstands at topographic highs and enhance RSL rise rates in grabens (Drachev, 1998; Imaev et al., 2000). The anomalously high position of RSL in Western Siberia could also be partly explained by tectonic uplift, although few to no GPS or repeated leveling measurements are available to provide additional evidence.

In formerly glaciated areas, despite a strong GIA background signal, regional-scale tectonic movements might also be inferred from comparisons of RSL curves from adjacent regions. For example, Rugozerskiy Peninsula (Region 8, Fig. 4) is characterized by the most active Holocene uplift in the Russian Arctic, although glacio-isostatic rebound should have been stronger in Kandalaksha (Region 6. Fig. 4) and Lesozavodskiy (Region 7, Fig. 4) due to thicker LGM ice (Clason et al., 2014; Svendsen et al., 2004) and, possibly, later deglaciation (Hughes et al., 2016). Regional and local scale tectonic movements can also create scatter in RSL records of a single site or small region. For example, the tectonic uplift of the same Rugozerkiy Peninsula (Region 8) is complicated by local-scale differential movements. Two lakes that were simultaneously isolated from the sea at ~9.3 ka are now situated at elevations of 87 and 72 m (Fig. 4, Region 8; Romanenko and Shilova, 2012), which implies a 0.5 m/kyr difference in rates of RSL fall since 9.3 ka. A similar discrepancy is observed in Chupa (Region 9, Fig. 4) where two lakes isolated at 6.3 ka are now at 33 and 40 m (Kolka et al., 2015). The drivers of such differential movements are active modern tectonics of the Kandalaksha Gulf, occupied by the Kandalaksha graben, part of the seismically active White Sea Rift system (Amantov et al., 2000a, b; Baluev et al., 2009a, b; see Fig. 3). Active movements along two large faults that feather this system,

Rugozerskaya Bay and Chupa Bay Faults (Baranskaya, 2015), cause discrepancy in the RSL data in Regions 8 and 9.

Differences in the shapes of the Murman coast RSL curves (Regions 1–3, Fig. 4), especially noticeable in the Mid-Holocene, may be caused by the influence of a large seismically active fault, the Karpinskiy Lineament (Baluev et al., 2016; Nikolaeva et al., 2007, Fig. 3), stretching along the Murman coast. In addition, the scatter of the Franz-Josef Land (Region 20) data at the beginning of the Holocene probably also resulted from different rates of crustal block movements (Gusev et al., 2013a).

6. Conclusions

We have constructed the first quality-controlled, post-LGM RSL database spanning the Russian Arctic using multiple sea-level indicators. For the first time, standardized methodology of database construction, data quality and uncertainties' estimation was employed. This made RSL histories from different indicators and different locations broadly comparable, and allowed us to identify broad-scale patterns of change in response to ESL, GIA-driven changes from Eurasian ice sheet complex, and tectonic processes operating over different spatial scales.

It has been established that first-order patterns of RSL change are driven by GIA response to Eurasian ice sheet complex. For territories of the former LGM Eurasian ice sheet, three RSL patterns were discovered: a) constant RSL fall (Baltic Shield, Franz-Josef Land, Novaya Zemlya); b) early post-LGM RSL rise to a highstand and subsequent Holocene RSL fall (western White Sea coasts); and c) early to mid-Holocene RSL lowstand, followed by a rise and a highstand (north-western Russian Plain). These patterns depended on LGM ice sheet thickness, deglaciation rates and history and paleogeographic conditions (such as the presence of proglacial White Sea Ice lake). An important finding is the identification of vertical tectonic movements in RSL records of regions with intense GIA (e.g., the Baltic shield), on a global, regional and local scale.

- In the intermediate-field areas (Timan coast, Kara Sea shelf), sparse data provides evidence of proglacial forebulge collapse, but does not allow estimation of its spatial extent and timing. Yamal and Gydan Peninsula and Severnaya Zemlya show anomalously high LGM RSL position, followed by an early Holocene lowstand and a late Holocene highstand of not more than several meters above modern sea-level.
- In far-field areas (Eastern Siberia), RSL rise was followed by a highstand eventually caused by signals from ocean syphoning, continental levering, perturbations to the Earth's rotation vector and other factors. Some of the existing discrepancies and scatter in the RSL data result from local differential block tectonic movements, the main reason being movements along faults of the Laptev Sea Rift System.

For more complete understanding of post-LGM RSL changes and their driving factors, better resolution in the data coverage is needed. While the western part of the Russian Arctic in formerly glaciated areas has the most complete RSL records, intermediate-field areas, especially the West Siberian Platform, as well as the whole Siberian Arctic, remain a challenge for future RSL studies. New sea-level indicators in these regions will permit a more comprehensive understanding of the mechanisms, timing and patterns of post-LGM RSL changes in the Russian Arctic.

7. Data availability

The database originating from our research is included as a supplementary material to the present manuscript.

Declarations of interest

None.

Acknowledgements

A.V.B. is supported by the RFBR project 16-35-60118 mol_a_dk, F.A.R. is supported by the State Budget Theme of the Laboratory of Geoecology of the North, Faculty of Geography, MSU АААА-А16-116032810055-0; B.P.H., N.S.K. and K.R. are supported by Singapore Ministry of Education Academic Research Fund Tier 1 RG119/17 and National Research Foundation Singapore and the Singapore Ministry of Education under the Research Centers of Excellence initiative. W.R.P. is funded by NSERC Discovery Grant A9627. This work is a contribution to IGCP (International Geoscience Programme) Project 639 and. PALSEA2 (Palaeo-Constraints on Sea-Level Rise). This is Earth Observatory of Singapore contribution 203.

Appendix A. Supplementary data

Supplementary data related to this article can be found at https://doi.org/10.1016/j.quascirev.2018.07.033.

References

Afanasenkov, A.P., Nikishin, A.M., Unger, A.V., Bordunov, S.I., Lugovaya, O.V., Chikisheva, A.A., Yakovishina, E.V., 2016. The tectonics and stages of the geological history of the Yenisei–Khatanga basin and the conjugate Taimyr orogeny. J. Geotectonics 50 (2), 23–42. http://doi.org/10.1134/S0016852116020023.

Aitken, M.J., 1998. An Introduction to Optical Dating. Oxford University Press, Oxford, p. 262.

Amantov, A.V., Zhamoyda, V.A., Manuylov, S.F., Moskalenko, P.E., Petrov, B.V., Spiridonov, M.A., Yakobson, K.E., 2000a. Geological Atlas of the White Sea. Electronic Publication of VSEGEI (All-Russian Geologic Institute Named after A.P. Karpinskiy). Cartographic fabric of VSEGEI, Saint-Petersburg (In Russian).

Amantov, A.V., Zhamoyda, V.A., Manuylov, S.F., Moskalenko, P.E., Petrov, B.V., Spiridonov, M.A., Yakobson, K.E., 2000b. Geological Atlas of the White Sea. Thickness Map of the White Sea and Adjacent Land Quaternary Deposits. Electronic Publication of VSEGEI (All-Russian Geologic Institute Named after A.P. Karpinskiy). Cartographic fabric of VSEGEI, Saint-Petersburg (In Russian).

Andreev, A., Tarasov, P., Schwamborn, G., Ilyashuk, B., Ilyashuk, E., Bobrov, A., Klimanov, V., Rachold, V., Hubberten, H.W., 2004. Holocene paleoenvironmental records from Nikolay Lake, Lena River delta, Arctic Russia. Palaeogeogr. Palaeoclimatol. Palaeoecol. 209, 197–217. https://doi.org/10.1016/j.palaeo.2004.02.010.

Anisimov, M.A., Ivanova, V.V., Pushina, Z.V., Pitulko, V.V., 2009a. Lagoonal deposits of Zhokhov Island: age, formation conditions and meaning for regional paleogeographic reconstructions of New Siberian Islands. Izv.RAS Ser.Geogr. 5, 107–119 (In Russian).

Anisimov, M.A., Pavlova, E.Yu, Pitulko, V.V., 2009b. Holocene of the New Siberian Islands. Fundamental problems of the Quaternary: results of investigations and future perspectives. In: Proceedings of the VI All-Russian Quaternary Workshop. Novosibirsk, pp. 38–40 (In Russian).

Arslanov, KhA., Lavrov, A.S., Potapenko, L.M., Tertychnaya, T.V., 1987. New Data on Late Pleistocene and Early Holocene Geochronology and Paleogeography of the Northern Pechora lowland. New Data on Geochronology of the Quaternary. Nauka, Moscow, pp. 101–111 (In Russian).

Astakhov, V.I., Nazarov, D.V., 2010. The stratigraphy of the upper neopleistocene of western Siberia and its geochronometric justification. Regional'naja geologija i metallogenija 43, 36–47 (in Russian).

Astakhov, V., 2014. The postglacial Pleistocene of the northern Russian mainland. Quat. Sci. Rev. 92, 388–408. https://doi.org/10.1016/j.quascirev.2014.03.009.

Avetisov, G.P., 1996. Tectonic factors of the intra-plate seismicity of the western Arctic sector. Physics of the Earth 12, 59–71 (In Russian).

Baluev, A.S., Morozov, YuA., Terekhov, E.N., Bayanova, T.B., Tyupanov, S.N., 2016. Tectonics of the junction region between the East European craton and West Arctic platform. J. Geotectonics 50 (5), 453–481. http://doi.org/10.1134/S0016852116050022.

Baluev, A.S., Zhuravlev, V.A., Przhiyalgovskii, E.S., 2009a. New data on the structure of the central part of the White Sea paleorift system. Dokl. Earth Sci. 427, 891–896.

Baluev, A.S., Przhiyalgovskii, E.S., Terekhov, E.N., 2009b. New data on tectonics of Onega-Kandalaksha paleorift (the White Sea). Dokl. Earth Sci. 425, 249–252.

Baranskaya, A.V., 2015. The Role of the Latest Tectonic Movements in the Formation of the Relief of the Coasts of the Russian Arctic. Summary of the Thesis for a Degree of Doctor of Philosophy (Geographical Science), Speciality 25.00.25 -

Geomorphology and Evolutional Geography. PhD thesis. Saint Petersburg State University, Saint-Petersburg, p. 26 (In Russian).
Baranskaya, A.V., Bolshiyanov, D.Yu, Kuchanov, Yul., Tomashunas, V.M., 2013. New data on dislocations in the Quaternary deposits of the Yamal and Gydan peninsula and the latest tectonic movements associated with them by the results of the "Yamal-Arctic-2012" expedition. Probl. Arktiki Antarkt. 4 (98), 91–102 (in Russian).
Baranskaya, A.V., Romanenko, F.A., 2017. Differentiated Vertical Movements of the Earth's Crust at the Baltic Shield. Relevant Problems of Geology, Geophysics and Geoecology. XXVIII Scientific Youth Conference in Memory of K.O. Kratz. VVM Publishing House, Saint Petersburg, pp. 14–16 (In Russian).
Baranskaya, A.V., Romanenko, F.A., Arslanov, KhA., Maksimov, F.E., Starikova, A.A., Pushina, Z.V., 2018. Quaternary sediments of Beliy Island: stratigraphy, age and formation conditions. Earth's Cryosphere XXII (2), 3–15. https://doi.org/10.21782/KZ1560-7496-2018-2(3-15) (In Russian).
Basilyan, A.E., Nikolskiy, P.A., Maksimov, F.E., Kuznetsov, V.Yu, 2010. Age of Traces of Ice Sheets on New Siberian Islands Based on 230Th/U Dating of Mollusc Shells. Structure and History of the Lithosphere. Paulsen, Moscow, pp. 506–514 (In Russian).
Bauch, H.A., Kassens, H., Erlenkeuser, H., Grootes, P.M., Thiede, J., 1999. Depositional environment of the Laptev Sea (Arctic Siberia) during the Holocene. Boreas, Oslo 28, 194–204. https://doi.org/10.1111/j.1502-3885.1999.tb00214.x.
Bogdanov, Yu.B., Yakobson, K.E., Amantov, A.V., 2000. State geologic map of the Russian Federation (new series). Scale 1:1000000. List Q-(35)-37 (Kirovsk). In: Bogdanov, YuB. (Ed.), VSEGEI (All-Russian Geologic Institute Named after A.P. Karpinskiy). Cartographic Fabric of VSEGEI, Saint-Petersburg (In Russian).
Bolshiyanov, D.Yu, Anokhin, V.M., Gusev, E.A., 2006. New data on topography and Quaternary sediments of Novaya Zemlya archipelago. Geologic-geophysical characteristics of the Arctic lithosphere. Mater.VNII Okeangeologiya 210. Saint-Petersburg, 149-161. (In Russian).
Bolshiyanov, D.Yu, Makeev, V.M., 1995. Severnaya Zemlya Archipelago. Glaciations and Environmantal History. Gidrometeoizdat, Saint-Petersburg, p. 21 (In Russian).
Bolshiyanov, D.Yu, Makarov, A.S., Schneider, V., Stof, G., 2013. Origin and Evolution of the Lena Delta. Saint-Petersburg, the Arctic and Antarctic Research Institute Publishing House, p. 268 (In Russian).
Bolshiyanov, D.Yu, Pogodina, I.A., Gusev, E.A., Sharin, V.V., Alekseev, V.V., Dymov, V.A., Anokhin, V.M., Anikina, N.Yu, Derevianko, L.G., 2009. New data on coastlines of Franz-josef land, Novaya Zemlya and savlbard archipelagos. Probl. Arktiki Antarkt. (Probl. Arctic Antarct) 2 (82), 68–77 (In Russian).
Boyarskaya, T.D., Polyakova, E.I., Svitoch, A.A., 1986. New data on the White Sea Holocene transgression. Doklady USSR,Acad. Sci. 4, 964–968 (In Russian).
Burguto, A.G., Zhuravlev, V.A., Zavarzina, G.A., Zinchenko, A.G., et al., 2016. State Geologic Map of the Russian Federation. Scale 1:1000000 (Third Generation). Series Barents-North Kara. List S-(36), 37 - Barents Sea (Western and central Part). Explanatory Report. VSEGEI (All-Russian Geologic Institute Named after A.P. Karpinskiy). Cartographic Fabric of VSEGEI, Saint-Petersburg, p. 144 (In Russian).
Clark, J.A., Farrell, W.E., Peltier, W.R., 1978. Global changes in postglacial sea level: A numerical-calculation. Quat. Res. 9 (3), 265–287. https://doi.org/10.1016/0033-5894(78)90033-9.
Clark, P.U., Mitrovica, J.X., Milne, G.A., Tamasea, M.E., 2002. Sea level finger printing as a direct test of the source of meltwater pulse (1a). J. Sci. 295, 2438–2441. https://dx.doi.org/10.1126/science.1068797.
Clason, C.C., Applegate, P.J., Holmlund, P., 2014. Modelling Late Weichselian evolution of the Eurasian ice sheets forced by surface meltwater-enhanced basal sliding. J. Glaciol. 60 (219), 29–40. https://doi.org/10.3189/2014JoG13J037.
Corner, G.D., Kolka, V.V., Yevzerov, V.Y., Møller, J.J., 2001. Postglacial relative sea-level change and stratigraphy of raised coastal basins on Kola Peninsula, northwest Russia. Global Planet. Change 31, 155–177. https://doi.org/10.1016/S0921-8181(01)00118-7.
Corner, G.D., Haugane, E., 1993. Marine-lacustrine stratigraphy of raised coastal basins and postglacial sea-level change at Lyngen and Vanna, Troms, northern Norway. Nor. Geol. Tidsskr. 73, 175–197.
Corner, G.D., Yevzerov, V.Y., Kolka, V.V., Møller, J.J., 1999. Isolation basin stratigraphy and Holocene relative sea-level change at the Norwegian–Russian border north of Nikel, northwest Russia. Boreas 28, 146–166. https://doi.org/10.1111/j.1502-3885.1999.tb00211.x.
Demidov, I.N., Houmark-Nielsen, M., Kjaer, K.H., Funder, S., Larsen, E., Astrid, L., Lunkka, J.-P., Saarnisto, M., 2004. Valdaian glacial maxima in the Arkhangelsk district of northwestern Russia. Developments in Quaternary Sciences. Quaternary Glaciations-extent and Chronology, vol. 2. Elsevier. https://doi.org/10.1016/S1571-0866(04)80082-4. part 1, 321-336.
Demidov, I.N., Houmark-Nielsen, M., Kjaer, K.H., Larsen, E., 2006. The last Scandinavian Ice Sheet in northwestern Russia: ice flow patterns and decay dynamics. Boreas 35, 425–443. https://doi.org/10.1080/03009480600781883.
Drachev, S.S., Kaul, N., Beliaev, V.N., 2003. Eurasia spreading basin to Laptev Shelf transition: structural pattern and heat flow. Geophys. J. Int. 152, 688–698. https://doi.org/10.1046/j.1365-246X.2003.01882.x.
Drachev, S.S., Shkarubo, S.I., 2017. Tectonics of the Laptev Shelf, Siberian Arctic. Geological Society, London, Special Publications, p. 460. http://doi.org/10.1144/SP460.15.
Drachev, S.S., 1998. Laptev Sea rifted continental margin: modern knowledge and unsolved questions. Polarforschung Bremerhav.) Alfred Wegener Inst. Polar Mar. Res.Ger. Soc Polar Res. 68, 41–50.
Drachev, S.S., 2016. Fold belts and sedimentary basins of the Eurasian Arctic. Arktos 2, 21. http://doi.org/10.1007/s41063-015-0014-8.
Dredge, L.A., 1991. Raised marine features, radiocarbon dates, and sea level changes, eastern Melville peninsula, arctic Canada. Arctic 44 (1), 63–73.
Ekman, M., Mäkinen, J., 1996. A consistent map of the postglacial uplift of Fennoscandia. Terra. Nova 8, 158–165.
Engelhart, S.E., 2010. Sea-level Changes along the U.S. Atlantic Coast: Implications for Glacial Isostatic Adjustment Models and Current Rates of Sea-level Change. PhD thesis. University of Pennsylvania.
Engelhart, S.E., Horton, B.P., Kemp, A.C., 2011. Holocene sea level changes along the United States' Atlantic Coast. Oceanography 24 (2), 70–79. https://doi.org/10.5670/oceanog.2011.28.
Engelhart, S.E., Horton, B.P., 2012. Holocene sea level database for the Atlantic coast of the United States. Quat. Sci. Rev. 54, 12–25. https://doi.org/10.1016/j.quascirev.2011.09.013.
Engelhart, S.E., Horton, B.P., Kopp, R.E., Nelson, A.R., Vacchi, M., 2015. A sea-level database for the Pacific coast of central North America. Quat. Sci. Rev. 113, 78–92. https://doi.org/10.1016/j.quascirev.2014.12.001.
Forman, S.L., Ingolfsson, O., Gataullin, V., Manley, W., Lokrantz, H., 2002. Late Quaternary stratigraphy, glacial limits, and paleoenvironments of the Marresale area, western Yamal Peninsula, Russia. Quat. Res. (Duluth 57, 355–370. https://doi.org/10.1006/qres.2002.2322.
Forman, S.L., Lubinski, D.J., Ingolfsson, O., Zeeberg, J.J., Snyder, J.A., Siegert, M.J., Matishov, G.G., 2004. A review of postglacial emergence on Svalbard, Franz Josef Land and Novaya Zemlya, northern Eurasia. Quat. Sci. Rev. 23, 1391–1434. https://doi.org/10.1016/j.quascirev.2003.12.007.
Forman, S.L., Lubinski, D., Miller, G.H., Matishov, G.G., Korsun, S., Snyder, J., Herlihy, F., Weihe, R., Myslivets, V., 1996. Postglacial emergence of western Franz Josef Land, Russia and retreat of the Barents Sea ice sheet. Quat. Sci. Rev. 15, 77–99.
Forman, S.L., Lubinski, D.J., Miller, G.H., Snyder, J., Matishov, G.G., Korsun, S., Myslivets, V., 1995. Postglacial emergence and distribution of late Weichselian ice-sheet loads in the northern Barents and Kara seas, Russia. J. Geol. 23 (2), 113–116. http://doi.org/10.1130/0091-7613(1995)023. <0113:PEADOL>2.3.CO;2.
Forman, S.L., Lubinski, D.J., Zeeberg, J.J., Polyak, L., 1999. Postglacial emergence and late quaternary glaciation on northern Novaya Zemlya, arctic Russia. Boreas, Oslo 28, 133–145. http://doi.org/10.1111/j.1502-3885.1999.tb00210.x.
Forsström, P.-L., Sallasmaa, O., Greve, R., Zwinger, T., 2003. Simulation of fast-flow features of the Fennoscandian ice sheet during the Last Glacial Maximum. Ann. Glaciol. 37, 383–389. https://doi.org/10.3189/172756403781815500.
Franke, D., Hinz, K., Block, M., Drachev, S.S., Neben, S., Kosko, M.K., Reichert, C., Roeser, H.A., 1998. Tectonics of the Laptev Sea region in north-Eastern Siberia. Polarforschung 68, 51–58.
Gehrels, W.R., Milne, G.A., Kirby, J.R., Patterson, R.T., Belknap, D.l.F., 2004. Late Holocene sea-level changes and isostatic crustal movements in Atlantic Canada. Quat. Int. 120, 79–89. https://doi.org/10.1016/j.quaint.2004.01.008.
Gehrels, W.R., Long, A.J., 2007. Quaternary land-ocean interactions: sea-level change, sediments and tsunami. J. Mar. Geol. 242, 1–4. https://doi.org/10.1016/J.Margeo.2007.05.005.
Grigoriev, M.N., 1993. Cryomorphogenesis of the Mouth of the Lena River. Yakustk, Institute of Permafrost studies of the Siberian branch of the Russian Academy of Science, 176 pp. (In Russian).
Grigorieva, A.K., 1987. Palynological Characteristics of the Late Pleistocene Sediments of West-siberian Polar Regions. Summary of the Thesis for a Degree of Doctor of Philosophy (Geographical Science), Speciality 25.00.25 - Geomorphology and Evolutional Geography. PhD thesis. Lomonosov Moscow State University, Moscow, pp. 195–209 (In Russian).
Gusev, E.A., Bolshiyanov, D.Yu, Dymov, V.A., Sharin, V.V., Arslanov, KhA., 2013a. Holocene marine terraces of the southern Franz-Josef Land islands. Probl. Arktiki Antarkt.(Probl.Arctic Antarct.) 3 (97), 103–108 (In Russian).
Gusev, E.A., Anikina, N.Ju, Arslanov, KhA., Bondarenko, S.A., Derevjanko, L.G., Molod'kov, A.N., Pushina, Z.V., Rekant, P.V., Stepanova, G.V., 2013b. Quaternary sediments and palaeogeography of Sibiriakov Island in the last 50 kA. Proc. Russ. Geograph. Soc. 4 (145), 65–79 (in Russian).
Hijma, M.P., Engelhart, S.E., Tornqvist, T.E., Horton, B.P., Hu, P., Hill, D.F., 2015. A protocol for a geological sea-level database. In: Shennan, I., Long, A.J., Horton, B.P. (Eds.), Handbook of Sea-level Research. John Wiley & Sons, Ltd, New York, pp. 536–553.
Hindle, D., Fujita, K., Mackey, K., 2006. Current deformation rates and extrusion of the northwestern Okhotsk plate, northeast Russia. Geophys. Res. Lett. 33 https://doi.org/10.1029/2005GL024814. L02306.
Hindle, D., Mackey, K., 2011. Earthquake recurrence and magnitude and seismic deformation of the northwestern Okhotsk plate, northeast Russia. J. Geophys. Res. 116 https://doi.org/10.1029/2010JB007409. B02301.
Holmes, M.L., Creager, J.S., 1974. Holocene history of the Laptev Sea continental shelf. In: Herman, Y. (Ed.), Marine Geology and Oceanography of the Arctic Seas. Springer Berlin Heidelberg, pp. 211–229.
Horton, B.P., Kopp, R.E., Garner, A.J., Hay, C.C., Khan, N.S., Roy, K., Shaw, T.A., 2018. Mapping sea-level change in time, space, and probability. Annu. Rev. Environ. Resour. 43. https://doi.org/10.1146/annurev-environ-102017-025826.
Hughes, A.L.C., Gyllencreutz, R., Lohne, Ø.S., Mangerud, J., Svendsen, J.I., 2016. The last Eurasian ice sheets e.a. chronological database and time-slice reconstruction, DATED-1. Boreas 45, 1–45. https://doi.org/10.1111/bor.12142.
Imaev, V.S., Imaeva, L.P., Koz'min, V.M., 1995. Seismotectonic dislocations in seismic belts of Yakutia. Geotectonics (29), 73–86 (In Russian).

Imaev, V.S., Imaeva, L.P., Koz'min, V.M., 2000. Seismotectonics of Yakutia. GEOS, Moscow, p. 227 (In Russian).
Ivanov, K.S., Erokhin, Y.V., Ponomarev, V.S., Pogromskaya, O.E., Berzin, S.V., 2016. Geological structure of the basement of western and eastern parts of the west-Siberian plain. Int. J. Environ. Sci. Educ. 11 (14), 6409–6432. ISSN EISSN-1306-3065.
Kaplin, P.A., Selivanov, A.O., 1999. Changes in the Level of the Russian Seas and Coastal Evolution: Past, Present, Future. GEOS, Moscow, p. 289 (in Russian).
Khan, N.S., Ashe, E., Horton, B.P., Dutton, A., Kopp, R.E., Brocard, G., Engelhart, S.E., Hill, D.F., Peltier, W.R., Vane, C.H., Scatena, F.N., 2017. Drivers of Holocene Sea-level change in the caribbean. Quat. Sci. Rev. 155, 13–36. https://doi.org/10.1016/j.quascirev.2016.08.032.
Khain, V.E., Filatova, N.I., 2007. Main stages in tectonic evolution of the Eastern Arctic region. Dokl. Earth Sci. 415 (2), 850–855. https://doi.org/10.1134/S1028334X07060050.
Kolka, V.V., Korsakova, O.P., 2010. Age of archaeological stone labyrinths and relative movement of White Sea's strand line in late-glacial and Holocene epochs. Proc. Russ. Geogr. Soc. 142 (1), 52–63 (In Russian).
Kolka, V.V., Evzerov, V.Ya, Møller, J.J., Corner, G.D., 2005. In: Mitrofanov, F.P. (Ed.), Postglacial Glacioisostatic Movements in the north-east of the Baltic Shield. New Data on Geology and mineral Resources of Kola Peninsula (Collected Essays). Kola Research Center of the Russian Academy of Sciences Publishing house, Apatity, pp. 15–25 (In Russian).
Kolka, V.V., Evzerov, V.Ya, Møller, J.J., Corner, G.D., 2013a. Late Pleistocene-Holocene sea level changes and bottom sediment stratigraphy of isolated lakes in the southern Kola Peninsula, area of Umba settlement. Izv.RAS Ser.Geogr. (1), 73–88 (In Russian).
Kolka, V.V., Korsakova, O.P., Shelekhova, T.S., Lavrova, N.B., Arslanov, KhA., 2013b. Reconstruction of the relative position of the White Sea in the Holocene on the Karelian coast (Engozero settlement district, northern Karelia). Doklady Russ. Acad. Sci. 449 (5), 587–592 (In Russian).
Kolka, V.V., Korsakova, O.P., Shelekhova, T.S., Tolstobrova, A.N., 2015. Reconstruction of the relative level of the White Sea during the Lateglacial – Holocene according to lithological, diatom analyses and radiocarbon dating of small lakes bottom sediments in the area of the Chupa settlement (North Karelia, Russia). Vestnik of MGTU 18 (2), 255–268 (In Russian).
Konechnaya, Y.V., 2013. Seismic analysis around Franz josef land. Vestnik of northern (arctic) federal university, series natural sciences. NAFU, Arkhangelsk (1), 10–13 (In Russian).
Koshechkin, B.I., 1979. Holocene Tectonics of the Eastern Baltic Shield. Nauka, Leningrad, p. 158 (In Russian).
Krapivner, R.B., 2006. Quick subsidence of the Barents shelf in the last 15-16 kA. Geotectonics (3), 39–51 (In Russian).
Lambeck, K., Chappell, J., 2001. Sea level change through the last glacial cycle. J. Sci. 292 (5517), 679–686. https://doi.org/10.1126/science.1059549.
Lambeck, K., Rouby, H., Purcell, A., Sun, Y., Sambridge, M., 2014. Sea level and global ice volumes from the last glacial maximum to the Holocene. Proc. Natl. Acad. Sci. Unit. States Am. 111, 15296–15303. https://doi.org/10.1073/pnas.1411762111.
Lambeck, K., Yokoyama, Y., Purcell, A., 2002. Into and out of the Last Glacial Maximum: sea-level change during Oxygen Isotope Stages 3 and 2. Quat. Sci. Rev. 21, 343–360. https://doi.org/10.1016/S0277-3791(01)00071-3.
Larsen, E., Kjaer, K.H., Demidov, I.N., Funder, S., Grosfjeld, K., Houmark-Nielsen, M., Jensen, M., Linge, H., Lysa, A., 2006. Late Pleistocene glacial and lake history of northwestern Russia. Boreas 35, 394–424. https://doi.org/10.1080/03009480600781958 .
Lavrov, A.S., Potapenko, L.M., 2005. The Neopleistocene of the north-eastern Russian Plain. Aerogeology, Moscow, p. 222 (In Russian).
Levitan, M.A., Lavrushin, Yu.A., Stein, R., 2007. Essays on the History of Sedimentation in the Arctic Ocean and Sub-arctic Seas during the Last 130 Ka. GEOS, Moscow, p. 404 (In Russian).
Long, A.J., Woodroffe, S.A., Roberts, D.H., Dawson, S.A., 2011. Isolation basins, sea-level changes and the Holocene history of the Greenland Ice Sheet. Quat. Sci. Rev. 30, 3748–3768. https://doi.org/10.1016/j.quascirev.2011.10.013.
Lukashov, A.A., Romanenko, F.A., 2010. Features and morphodynamics of the disjunctive north-eastern border of the Baltic shield ("Karpinskiy line"). Tectonics and geodynamics of Phanerozoic fold systems and platforms. In: Proceedings of the XLIII Tectonic Workshop, vol. 1. GEOS, Moscow, p. 448 (in Russian).
Lunkka, J.-P., Putkinen, N., Miettinen, A., 2012. Shoreline displacement in the Belomorsk area, NW Russia during the younger Dryas stadial. Quat. Sci. Rev. 37, 26–37. https://doi.org/10.1016/j.quascirev.2012.01.023.
Makarov, A.S., 2009. Changes in the Laptev Sea Level as a Factor if Lena Delta Formation in the Holocene. Summary of the Thesis for a Degree of Doctor of Philosophy (Geographical Science), Speciality 25.00.25 - Geomorphology and Evolutional Geography. PhD thesis. Saint Petersburg State University, Saint-Petersburg, p. 16 (In Russian).
Makarov, A.S., 2017. Changes in the Level of Arctic Seas in the Holocene. Summary of a Dr. Hab. Thesis in Geographical Science Summary of the Thesis for a Degree of Doctor of Philosophy (Geographical Science), Speciality 25.00.25 - Geomorphology and Evolutional Geography. PhD thesis. Saint Petersburg State University, Saint-Petersburg, p. 45 (In Russian).
Makeev, V.M., 1988. Fluctuations of the Gulf of Ob Level in the Holocene. Geographical and Glaciological Investigations in Polar Regions. Gidrometeoizdat, Leningrad, pp. 137–146 (In Russian).
Milne, G.A., Gehrels, W.R., Hughes, C.W., Tamisiea, M.E., 2009. Identifying the causes of sea-level change. Nat. Geosci. 2, 471–478. https://doi.org/10.1038/ngeo544.
Milne, G.A., Mitrovica, J.X., 1998. Postglacial sea-level change on a rotating Earth. J. Geophys. 133, 1–19. https://doi.org/10.1046/j.1365- 246X.1998.1331455.x.
Milne, G.A., Mitrovica, J.X., 2008. Searching for eustasy in deglacial sea-level histories. Quatern. Sci. Rev. 27, 2292–2302. https://doi.org/10.1016/j.quascirev.2008.08.018.
Mints, M.V., Dokukina, K.A., Konilov, A.N., Philippova, I.B., Zlobin, V.L., Babayants, P.S., Belousova, E.A., Blokh, Y.I., Bogina, M.M., Bush, W.A., Dokukin, P.A., Kaulina, T.V., Natapov, L.M., Piip, V.B., Stupak, V.M., Suleimanov, A.K., Trusov, A.A., Van, K.V., Zamozhniaya, N.G., 2015. East European Craton: early precambrian history and 3D models of deep crustal structure. Geol. Soc. Am. Spec. Pap. 510, 433. https://doi.org/10.1130/SPE510.
Mitrovica, J.X., Peltier, W.R., 1991. On postglacial geoid subsidence over the equatorial oceans. J. Geophys. Res. Solid Earth 96 (Issue B12), 20053–20071. https://doi.org/10.1029/91JB01284.
Møller, J.J., Yevzerov, V.Ya, Kolka, V.V., Corner, G.D., 2002. Holocene raised beach-ridges and sea-ice pushed boulders on Kola Peninsula, Northwest Russia: indicators of climatic change. Holocene 12 (2), 169–176. http://doi.org/10.1191/0959683602hl532rp.
Møller, P., Lubinski, D.J., Ingolfsson, O., Forman, S.L., Seidenkrantz, M.-S., Bolshiyanov, D. Yu, Lokrantz, H., Antonov, O., Pavlov, M., Ljung, K., Zeeberg, J., Andreev, A., 2006. Severnaya Zemlya, arctic Russia: a nucleation area for Kara Sea ice sheets during the middle to late quaternary. Quat. Sci. Rev. 25 (21–22), 2894–2936. http://doi.org/10.1016/quascirev.2006.02.016.
Murray, A.S., Marten, R., Johnston, A., Martin, P., 1987. Analysis for naturally occurring radionuclides at environmental concentrations by gamma spectrometry. J. Radioanal. Nucl. Chem. 115, 263–288. http://doi.org/10.1007/BF02037443.
Murray, A.S., Wintle, A.G., 2000. Luminescence dating of quartz using an improved single aliquot regenerative-dose protocol. Radiat. Meas. 32, 57–73. http://doi.org/10.1016/S1350-4487(99)00253-X.
Musatov, E.E., 1996. Neotectonics of the Arctic continental margins. Physics of the Earth (12), 72–78 (In Russian).
Nikonov, A.A., 1977. Holocene and Modern Movements of the Earth's Crust. Nauka, Moscow, p. 240 (In Russian).
Nikolaev, N.I., 1988. Neotectonics and Geodynamics of the Lithosphere. Nedra, p. 291 (In Russian).
Nikolaeva, S.B., 2016. Seismically Induced Structures in Quaternary Sediments of the Fennoscandian Shield: Features and Age Constraints, 1. Vestnik of MGTU, Moscow, pp. 110–122 (In Russian).
Nikolaeva, S.B., Evzerov, V.Ya, Petrov, S.I., 2007. Seismic Features of the Landscape in the north-western Murmansk Region. North-2007. Kola Research Centre of the Russian Academy of Sciences Publishing House, Apatity, p. 12 (In Russian).
Olley, J.M., Murray, A.S., Roberst, R.G., 1996. The effects of disequilibria in uranium and thorium decay chains on burial dose rates in fluvial sediments. Quat. Sci. Rev. 15 (7), 751–760. http://doi.org/10.1016/0277-3791(96)00026-1.
Patton, H., Hubbard, A., Andreassen, K., Auriac, A., Whitehouse, P.L., Stroeven, A., Shackleton, C., Winsborrow, M., Heyman, J., Hall, A., 2017. Deglaciation of the Eurasian ice sheet complex. Quat. Sci. Rev. 169, 148–172. https://doi.org/10.1016/j.quascirev.2017.05.019.
Pease, V., Drachev, S., Stephenson, R., Zhang, X., 2014. Arctic lithosphere — a review. Tectonophysics 628, 1–25. http://doi.org/10.1016/j.tecto.2014.05.033.
Peltier, W.R., 1976. Glacial isostatic adjustments - II: the inverse problem. Geophys. J. Roy. Astron. Soc. 46 (3), 605–646. http://doi.org/10.1111/j.1365-246X.1976.tb01253.x.
Peltier, W.R., 1998. Postglacial variations in the level of the sea: Implications for climate dynamics and solid- Earth geophysics. Rev. Geophys. 36 (Issue 4), 603–689. https://doi.org/10.1029/98RG02638.
Peltier, W.R., 2002. On eustatic sea level history: last glacial maximum to Holocene. Quat. Sci. Rev. 21 (1), 377–396. http://doi.org/10.1016/S0277-3791(01)00084-1.
Peltier, W.R., 2004. Global glacial isostasy and the surface of the ice-age Earth: the ICE-5G (VM2) model and GRACE. Annu. Rev. Earth Planet Sci. 32, 111–149. https://doi.org/10.1146/annurev.earth.32.082503.144359.
Peltier, W.R., Argus, D.F., Drummond, R., 2015. Space geodesy constraints ice age terminal deglaciation: the global ICE-6G_C (VM5a) model. J. Geophys. Res. Solid Earth 120. https://doi.org/10.1002/2014JB011176, 2014JB011176.
Peltier, W.R., Argus, D.F., Drummond, R., 2018. Comment on "An assessment of the ICE-6G_C (VM5a) Glacial Isostatic Adjustment Model" by Purcell et al. J. Geophys. Res.: Solid Earth 123, 2019-2018. https://doi.org/10/1002/2016JB013844.
Peltier, W.R., Farrell, W.E., Clark, J.A., 1978. Glacial isostasy and relative sea level: a global finite element model. Tectonophysics 50, 81–110. https://doi.org/10.1016/0040-1951(78)90129-4.
Polyak, L., Gataullin, V., Okuneva, O., Stelle, V., 2000. New constraints on the limits of the Barents-Kara ice sheet during the Last Glacial Maximum based on borehole stratigraphy from the Pechora Sea. J. Geology 28 (7), 611–614. https://doi.org/10.1130/0091-7613(2000)28<611:NCOTLO>2.0.CO;2.
Polyakova, E.I., Bauch, H.A., Klyuvitkina, T.S., 2005. Early to middle Holocene changes in Laptev Sea water masses deduced from diatom and aquatic palynomorph assemblages. Global Planet. Change 48 (1–3). https://doi.org/208–222. 10.1016/j.gloplacha.2004.12.014.
Polyakova, Y., Stein, R., 2004. Holocene paleoenvironmental implications of diatom and organic carbon records from the southeastern Kara Sea (Siberian Margin). Quat. Res. 62, 256–266. https://doi.org/10.1016/j.yqres.2004.08.002.
Preuss, H., 1979. Progress in computer evaluation of sea level data within the IGCP

project No. 61. In: Presented at the 1978 International Symposium on Coastal Evolution in the Quaternary. Universiade Sao Paulo, Sao Paulo, pp. 104–134.
Proshutinsky, A., Ashik, I.M., Dvorkin, E.N., Häkkinen, S., Krishfield, R.A., Peltier, W.R., 2004. Secular sea level change in the Russian sector of the Arctic Ocean. J. Geophys. Res. 109. https://doi.org/10.1029/2003JC002007.
Raab, A., Melles, M., Berger, G.W., Hagedorn, B., Hubberten, H.-W., 2003. Non-glacial paleoenvironments and the extent of Weichselian ice sheets on Severnaya Zemlya, Russian High Arctic. Quat. Sci. Rev. 22, 2267–2283. https://doi.org/10.1016/S0277-3791(03)00139-2 .
Reimer, P.J., Bard, E., Bayliss, A., Beck, J.W., Blackwell, P.G., Ramsey, C.B., Buck, C.E., Cheng, H., Edwards, R.L., Friedrich, M., Grootes, P.M., Guilderson, T.P., Haflidason, H., Hajdas, I., Hatté, C., Heaton, T.J., Hoffmann, D.L., Hogg, A.G., Hughen, K.A., Kaiser, K.F., Kromer, B., Manning, S.W., Niu, M., Reimer, R.W., Richards, D.A., Scott, E.M., Southon, J.R., Staff, R.A., Turney, C.S.M., Plicht, J., 2013. IntCal13 and Marine13 radiocarbon age calibration curves 0–50,000 Years cal. BP. Radiocarbon 55 (4), 1869–1887. https://doi.org/10.2458/azu_js_rc.55.16947.
Repkina, T.Yu, Romanenko, F.A., Baranskaya, A.V., Samsonova, S. Yu, 2018. Dynamics of the Eastern Coast of Unskaya Bay, White Sea in the Holocene. Vestnik MSU, Series Geography (submitted for publication) (In Russian).
Romanenko, F.A., Baranskaya, A.V., Ermolov, A.A., Kokin, O.V., 2015. Low Coasts of the Western Arctic Seas, vol. 140. Voprosy geografii, Moscow, pp. 275–306 (In Russian).
Romanenko, F.A., Shilova, O.S., 2012. Post-glacial uplift of the Karelian coast (White Sea) based on radiocarbon and diatom analyses of lacustrine and boggy sediments of Kindo Peninsula. Dokl. Earth Sci. 442 (4), 544–548. https://doi.org/10.1134/S1028334X12020079.
Roy, K., Peltier, W.R., 2017. Space-geodetic and water level gauge constraints on continental uplift and tilting over North America: regional convergence of the ICE-6G C (VM5a/VM6) models. Geophys. J. Int. 210 (2), 1115–1142. https://doi.org/10.1093/gji/ggx156.
Schirrmeister, L., Kunitsky, V., Grosse, G., Wetterich, S., Meyer, H., Schwamborn, G., Babiy, O., Derevyagin, A., Siegert, C., 2011. Sedimentary characteristics and origin of the late Pleistocene Ice Complex on north-east Siberian Arctic coastal lowlands and islands - a review. Quat. Int. 241 (1–2), 3–25. https://doi.org/10.1016/j.quaint.2010.04.004.
Shennan, I., 1989. Holocene crustal movements and sea-level changes in Great Britain. J. Quat. Sci. 4 (1), 77–89. https://doi.org/10.1002/jqs.3390040109.
Shennan, I., Innes, J., Long, A., Zong, Y., 1995. Late Devensian and Holocene relative sea-level changes in northwestern Scotland: new data to test existing models. Quat. Int. 26, 97–123. http://doi.org/10.1016/1040-6182(94)00050-F.
Shipilov, E.V., Tiuremnov, V.A., Glaznev, V.N., Golubev, V.A., 2006. Paleogeographical conditions and tectonic deformations of the Barents continental margin in the Cenozoic. Doklady Russ. Acad. Sci. 407 (3), 378–383 (In Russian).
Siegert, M.J., Dowdeswell, J.A., Melles, J.A., 1999. Late Weichselian glaciation of the Russian High Arctic. Quat. Res. 53, 273–285. https://doi.org/10.1006/qres.1999.2082.
Simon, K., James, T., Forbes, D., Telka, A., Dyke, A., Henton, J., 2014. A relative sea-level history for arviat, nunavut, and implications for Laurentide ice sheet thickness west of Hudson Bay. Quat. Res. 82 (1), 185–197. https://doi.org/10.1016/j.yqres.2014.04.002.
Slabunov, A.I., Lobach-Zhuchenko, S.B., Bibikova, E.V., Balagansky, V.V., Sorjonen-Ward, P., Volodichev, O.I., Shchipansky, A.A., Svetov, S.A., Chekulaev, V.P., Arestova, N.A., Stepanov, V.S., 2006. The Archean of the Baltic Shield: geology, geochronology, and geodynamic settings. J. Geotectonics 40 (6), 409–433. http://doi.org/10.1134/S001685210606001X.
Snyder, J.A., Forman, S.L., Mode, W.N., Tarasov, G.A., 1997. Postglacial relative sea-level history: sediment and diatom records of emerged coastal lakes, north-central Kola Peninsula, Russia. Boreas, Oslo 26 (4), 329–346. http://doi.org/10.1111/j.1502-3885.1997.tb00859.x.
Stein, S., Sella, F., 2002. Plate boundary zones: concept and approaches. In: Stein, S, S., Freymueller, J. (Eds.), Plate Boundary Zones. Geodynamics, Series 30. AGU, Washington, D.C, ISBN 978-0-875-90532-7, pp. 1–26.
Stolbov, N.M., 2000. Specific features of Franz-Josef land archipelago magmatism as a reflection of its geodynamic features. In: Geologic and Geophysic Characteristics of the Arctic Lithosphere, vol. 3. VNIIOkeangeologiya, Saint-Petersburg, pp. 137–144 (In Russian).
Stroeven, A.P., Hättestrand, C., Kleman, J., Heyman, J., Fabel, D., Fredin, O., Goodfellow, B.W., Harbo, J.M.R., Jansen, J.D., Olsen, L., Caffee, M.W., Fink, D., Lundqvist, J., Rosqvist, G.C., Strömberg, B., Jansson, K.N., 2016. Deglaciation of Fennoscandia. Quat. Sci. Rev. 147, 91–121. http://doi.org/10.1016/j.quascirev.2015.09.016.
Svendsen, J.I., Alexanderson, H., Astakhov, V.I., Demidov, I., Dowdeswell, J.A., Funder, S., Gataullin, V., Henriksen, M., Hjort, C., Houmark-Nielsen, M., Hubberten, H.W., Ingolfsson, O., Jakobsson, M., Kjær, K.H., Larsen, E., Lokrantz, H., Lunkka, J.P., Lyså, A., Mangerud, J., Matiouchkov, A., Murray, A., Möller, P., Niessen, F., Nikolskaya, O., Polyak, L., Saarnisto, M., Siegert, C., Siegert, M.J., Spielhagen, R.F., Stein, R., 2004. Late Quaternary ice sheet history of northern Eurasia. Quat. Sci. Rev. 23, 1229–1271. https://doi.org/10.1016/j.quascirev.2003.12.008.
Stuiver, M., Polach, H.A., 1977. Discussion Reporting of 14C data. Radiocarbon 19 (3), 355–363. http://doi.org/10.1017/S0033822200003672.
Törnqvist, T.E., González, J.L., Newsom, L.A., Van der Borg, K., De Jong, A.F.M., Kurnik, C.W., 2004. Deciphering Holocene Sea-level history on the us gulf coast: a high-resolution record from the Mississippi delta. Geol. Soc. Am. Bull. 116 (7). http://doi.org/1026–1039. 10.1130/B2525478.1.
Törnqvist, T.E., Rosenheim, B.E., Hu, P., Fernandez, A.B., 2015. Radiocarbon dating and calibration. In: Shennan, I., Long, A.J., Horton, B.P. (Eds.), Handbook of Sealevel Research. John Wiley & Sons, Ltd., New York, pp. 347–360. http://doi.org/10.1002/9781118452547.ch23.
Tumskoy, V.E., 2012. Features of cryolithogenesis of the northern Yakoutia deposits in late neopleistocene-holocene. Earth's Cryosphere XVI, 12–21 (In Russian).
Van de Plassche, O., 1995. Evolution of the intra-coastal tidal range in the Rhine-Meuse delta and Flevo Lagoon, 5700-3000 yrs cal B.C. J. Mar. Geol., Coast. Evol. Quaternary IGCP Proj. 274 (124), 113–128. https://doi.org/10.1016/0025-3227(95)00035-W.
Vernikovsky, V.A., Dobretsov, N.L., Metelkin, D.V., Matushkin, N.Yu, Koulakov, I.Yu, 2013. Concerning tectonics and the tectonic evolution of the Arctic. Russ. Geol. Geophys. 54 (8), 838–858. http://doi.org/10.1016/j.rgg.2013.07.006.
Vink, A., Steffen, H.,L., Reinhard, L., Kaufmann, G., 2007. Holocene relative sea-level change, isostatic subsidence and the radial viscosity structure of the mantle of northwest Europe (Belgium, The Netherlands, Germany, southern North Sea). Quat. Sci. Rev. 26, 3249–3275. https://doi.org/10.1016/j.quascirev.2007.07.014.
Vinogradov, A.N., Baranov, S.V., Vinogradov, YuA., Asming, V.E., 2006. Seismic zones of the northern part of the Baltic shield. Active geological and geophysical processes in the lithosphere. Methods, means and results of investigations. In: Proceedings of the XII International Conference, 18-23 September 2006, vol. 1. Voronezh State University Publishing House, Voronezh, pp. 115–120 (In Russian).
Wetterich, S., Rudaya, N., Tumskoy, V., Andreev, A., Opel, T., Schirrmeister, L., Meyer, H., 2011. Last Glacial Maximum records in permafrost of the East Siberian Arctic. Quat. Sci. Rev. 30, 3139–3151. http://doi.org/10.1016/j.quascirev.2011.07.020.
Winterfeld, M., Schirrmeister, L., Grigoriev, M.N., Kunitsky, V.V., Andreev, A., Murray, A., Overduin, P.P., 2011. Coastal permafrost landscape development since the late Pleistocene in the western Laptev Sea, Siberia. Boreas 697–713. https://doi.org/10.1111/j.1502-3885.2011.00203.x. ISSN 0300-9483.
Woodroffe, S.A., Long, A.J., Lecavalier, B.S., Milne, G.A., Bryant, C.L., 2014. Using relative sea-level data to constrain the deglacial and Holocene history of southern Greenland. Quat. Sci. Rev. 92, 345–356. https://doi.org/10.1016/j.quascirev.2013.09.008.
Wu, P., Peltier, W.R., 1984. Pleistocene deglaciation and the Earth's rotation - a new analysis. Geophys. J. Roy. Astron. Soc. 76 (Issue 3), 753–791. https://doi.org/10.1111/j.1365-246X.1984.tb01920.x.
Young, N.E., Schaefer, J.M., Briner, J.P., Goehring, B.M., 2013. A 10Be production-rate calibration for the Arctic. J. Quat. Sci. 28, 515–526. https://doi.org/10.1002/jqs.2642.
Zaretskaya, N.E., Simakova, A.N., Sulerzhitsky, L.D., Shevchenko, N.V., 2011. Chronology of the North Dvina River delta development over the Holocene. Geochronometria 38 (2), 116–127. https://doi.org/10.2478/s13386-011-0012-y.
Zeeberg, J., Lubinski, D.J., Forman, S.L., 2001. Holocene relative sea level history of Novaya Zemlya, Russia, and implications for Late Weichselian ice-sheet loading. Quat. Res. 56 (2), 218–230. http://doi.org/10.1006/qres.2001.2256.
Zhuravlev, V.A., Korago, E.A., Kostin, D.A., Zuykova, O.N., et al., 2013. State Geologic Map of the Russian Federation. Scale 1:1000000 (Third Generation). Series Barents-North Kara. List R-39, 40 - Kolguev Island - Karskie Vorota Strait. Explanatory Report. VSEGEI (All-Russian Geologic Institute Named after A.P. Karpinskiy. Cartographic Fabric of VSEGEI, Saint-Petersburg, p. 477 (In Russian).
Zweck, C., Huybrechts, P., 2005. Modeling of the northern hemisphere ice sheets during the last glacial cycle and glaciological sensitivity. J. Geophys. Res. 110, 24. https://doi.org/10.1029/2004JD005489. D07103.
Zykov, D.S., Poleshchuk, A.V., Nikonov, A.A., 2017. Morphostructure of the division zone between the Baltic Shield and the Western Arctic platform as an indicator of interaction of geodynamical systems. Geomorphology, No 2, 79–89 (In Russian).